ESA Climate Change Initiative
River Discharge Precursor
(RD_cci+)

D.2. Selection of river basins

Contract number: 4000139952/22/I-NB

Reference: CCI-DISCHARGE-0004

Version 1.1 – 23/05/2023

11 rue Hermès, Parc Technologique du Canal — 31520 Ramonville Saint-Agne, France
Tel +33 (0)5 61 39 47 00 Fax +33(0)5 61 75 10 14
www.cls.fr

CHRONOLOGY ISSUES

Issue	Date	Object	Written by
1.0	21 April	Final version	Laetitia Gal (HM)
1.1	23 May 23	Edits according to ESA feedback	Laetitia Gal (HM)

Checked by	S. Biancamaria - LEGOS	
Approved by	Alice Andral - CLS	
Authorized by	Clément Albergel - ESA	

DISTRIBUTION

Company	Names	Email
ESA	Clément Albergel	clement.albergel@esa.int
ESA	Jérôme Benveniste	Jerome.Benveniste@esa.int
CLS	Alice Andral	aandral@groupcls.com
CLS	Yann Bernard	ybernard@groupcls.com
CLS	Maxime Vayre	mvayre@groupcls.com
CLS	Daya Ceccone	dceccone@groupcls.com
CLS	Nicolas Taburet	ntaburet@groupcls.com
CNRM	Simon Munier	simon.munier@meteo.fr
EOLA	Elena Zakharova	zavocado@gmail.com
Hydromatters	Malik Boussaroque	malik.boussaroque@hydro-matters.fr
Hydromatters	Laetitia Gal	laetitia.gal@hydro-matters.fr

Hydromatters	Adrien Paris	adrien.paris@hydro-matters.fr
IRPI	Silvia Barbetta	silvia.barbetta@irpi.cnr.it
IRPI	Luca Brocca	luca.brocca@irpi.cnr.it
IRPI	Stefania Camici	stefania.camici@irpi.cnr.it
IRPI	Angelica Tarpanelli	angelica.tarpanelli@irpi.cnr.it
LEGOS-CNRS	Sylvain Biancamaria	sylvain.biancamaria@legos.obs-mip.fr
LEGOS-IRD	Fabrice Papa	fabrice.papa@ird.fr
Magellium	Gilles Larnicol	gilles.larnicol@magellium.fr
Magellium	Vanessa Pedinotti	vanessa.pedinotti@magellium.fr

LIST OF CONTENTS/SOMMAIRE

LIST OF TABLES AND FIGURES

Figure 39. On the left side, the basin (red area) with main drainage network (black line), the available altimetry OLTC data from different constellations (cross) and in-situ gauges stations from different catalogues (colors points). On the right side, timeline of available data (WSE and discharge) for each selected stations of interest.

Table 1. Characteristics of each selected basins

Table 2. Characteristics of each selected stations with position, river, drainage area, timestep, and period and sources of in-situ gauges.

Table 3. Characteristics of each selected stations with position, river, drainage area, timestep, and period and sources of in-situ gauges.

Table 4. Characteristics of each selected stations with position, river, drainage area, timestep, and period and sources of in-situ gauges.

Table 5. Characteristics of each selected stations with position, river, drainage area, timestep, and period and sources of in-situ gauges.

Table 6. Characteristics of each selected stations with position, river, drainage area, timestep, and period and sources of in-situ gauges.

Table 7. Characteristics of each selected stations with position, river, drainage area, timestep, and period and sources of in-situ gauges.

Table 8. Characteristics of each selected stations with position, river, drainage area, timestep, and period and sources of in-situ gauges.

Table 9. Characteristics of each selected stations with position, river, drainage area, timestep, and period and sources of in-situ gauges.

Table 10. Characteristics of each selected stations with position, river, drainage area, timestep, and period and sources of in-situ gauges.

Table 11. Characteristics of each selected stations with position, river, drainage area, timestep, and period and sources of in-situ gauges.

Table 12. Characteristics of each selected stations with position, river, drainage area, timestep, and period and sources of in-situ gauges.

Table 13. Characteristics of each selected stations with position, river, drainage area, timestep, and period and sources of in-situ gauges.

Table 14. Characteristics of each selected stations with position, river, drainage area, timestep, and period and sources of in-situ gauges.

Table 15. Characteristics of each selected stations with position, river, drainage area, timestep, and period and sources of in-situ gauges.

Table 16. Characteristics of each selected stations with position, river, drainage area, timestep, and period and sources of in-situ gauges.

Table 17. Characteristics of each selected stations with position, river, drainage area, timestep, and period and sources of in-situ gauges.

Table 18. Characteristics of each selected stations with position, river, drainage area, timestep, and period and sources of in-situ gauges.

Table 19. Characteristics of each selected stations with position, river, drainage area, timestep, and period and sources of in-situ gauges.

REFERENCE DOCUMENTS

URD: D.1 User Requirements Document for CCI River Discharge precursor project (CCI-Discharge-0003-URD, Issue 1.0)

1 Introduction

As there is no global requirement for this CCI precursor project, time series will be identified for different basins around the globe. A subset of, at least, 15 river basins shall be considered. Similarly, discharge cannot be derived for the whole river network within the watershed, due to the lack of satellite data (especially for nadir altimetry) and availability of ancillary data compulsory to derive discharge (like in situ discharge time series).

This task will therefore define the criteria to select locations where the long time series of river discharge will be derived, based on the URD (especially on the “River basin coverage threshold” and “Locations threshold” requirements). These criteria will have to consider the need to have ECV for climate change studies. Therefore, these basins must be representative enough of global river streams and present contrasted geophysical and geomorphological conditions. We will choose around fifteen basins, with contrasted climate zones and sizes. Some of them should include natural or at least weakly anthropized streams to distinguish climatic trends from human-induced changes, and also large (> 1 km) and small (~ 100 m) stream. The choice also will be led by the availability of long-term in situ observations for the validation of project products. The project will include basins previously investigated by the different teams in order to get a much longer time series, but it will also include new unstudied basins.

Then, according to these criteria, the list of locations will be derived based also on:

- Availability of satellite observations (from nadir altimeters and multispectral imagers specified in section 5 of the URD) and ancillary data (especially in situ discharge time series).
- Availability of a previously calibrated MGB simulation for at least one of the selected basins
- A subset of basin will be selected and considered as “priority” basins that will be the first basins to be processed by the E0 team in WP3. These basins will be the first ones to be validated in WP4. “Priority” basins have been defined depending on different purposes:The basins on which the promoters have already worked allowing a consolidated knowledge of the in situ databases and the characteristics of the environmentThe basins with an available long term timeseries for discharge and water level. The basins with contrasted climate zone, geophysical and geomorphological features (at least one basin per continent)Among this subset, some locations (or basins) should have long discharge (and WSE) time series that cover the whole or almost the whole time period cover by the project (2002-2022, the URD “Time span threshold” requirement), so that we can calibrate over the same period all proposed methods (and test different assumption and methods especially due to the availability of ancillary discharge during the calibration phase) and validate all products over the same validation period.

The last task, once the dataset is ready, will be to split time series into two separate datasets, one for calibration and the other one for validation purpose.

2 Selection of basins

2.1 List of selected basins

A list of 18 basins have been selected to respond to all the issues and interests identified in the URD (Ref CCI-Discharge-0003-URD;Figure 1). The selected basins represent a wide diversity in terms of land use, land cover, anthropization, river width, drainage area, climate, data availability etc.

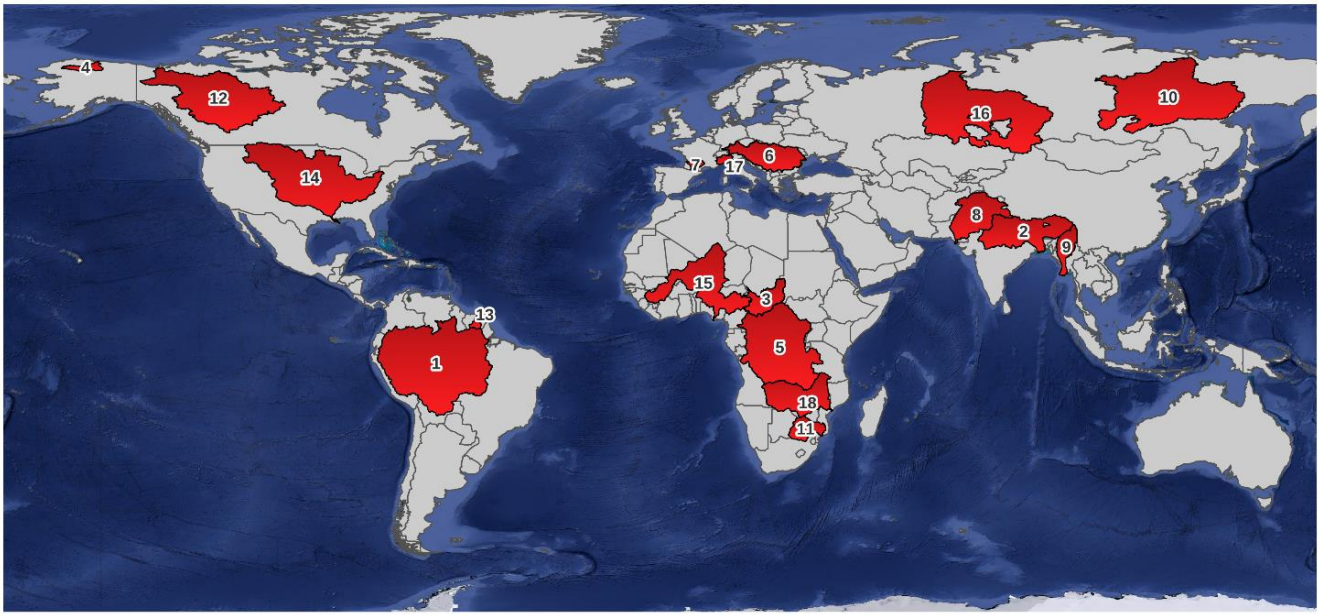

Selected basins

1 - AMAZON	4 - CONGO	7 - GARONNE	10 - LENA	13 - MARONI	16 - OB
2 - CHAD	5 - DANUBE	8 - INDUS	11 - LIMPOPO	14 - MISSISSIPPI	17 - PO
3 - COLVILLE	6 - GANGA-BRAHMAPUTRA	9 - IRRAWADDY	12 - MACKENZIE	15 - NIGER	18 - ZAMBEZI

Figure 1: All selected basins

Table 1 summarizes the characteristics of each selected basin in term of:

- Drainage area (km²),
- Mean discharge at the basin's outlet (m³/s),
- Main river length (m), based on Grill et al. (2019) classification,
- Percentage of free flowing, based on Grill et al. (2019) classification,
- Climatic zone, based on Köppen (1900) classification,
- Level of priority. The first to be processed are labelled "Tier 1", and the remaining are labelled "Tier 2".

n°	Basin name	Region	Area (km²)	Mean Q (m^3/s)	River Length *	% free flowing **	Relevance ***	Priority ****	Climatic zone *****
1	Amazon	South America	7.5 million	200 000	VL		1, 2, 3, 4	Tier 2	
2	Chad	Central Africa	608,500	1 250	VL		2,3,4	Tier 2	
3	Colville	Arctic	53 000	3 100	M		1,2,3,4,5	Tier 2	
4	Congo	Central Africa	3,7 million	40 000	VL		1, 2, 3, 4	Tier 1	
5	Danube	Europa	801 000	5 600	VL		1, 2, 3, 4	Tier 2	
6	Ganges-Brahmaputra	South Asia	2 million	32 000	L		1,2,3,4	Tier 2	
7	Garonne	Mid latitude	56 000	600	L		5	Tier 1	
8	Indus	South Asia	1.2 million	6 600	VL		2, 3	Tier 1	
9	Irrawaddy	South-eastern Asia	411 000	15 000	VL		2.4	Tier 2	
10	Lena	Arctic	2.5 million	16,500	VL		1, 2, 3, 4	Tier 2	
11	Limpopo	South Africa	415 000	400	L		2.4	Tier 2	
12	Mackenzie	Arctic	1,8 million	9 300	VL		2,3,4,5	Tier 2	
313	Maroni	South America	35 400	1 600	S		2,3,4	Tier 1	
14	Mississippi	North America	3.1 million	17 000	VL		2,3,4	Tier 1	
15	Niger	West Africa	2.1 million	6 900	L-VL		2,3,4	Tier 1	
16	Ob	Arctic	2.9 million	13 000	VL		2, 3	Tier 2	
17	Po	Mid latitude	74 000	1 500	L		5	Tier 1	
18	Zambesi	South Africa	1.4 million	3 900	L		2.4	Tier 2	

Table 1: Characteristics of each selected basins.

*: VL : Very long river (> 1000 km)
L : Long River (500-1000 km)
M: Medium River (100-500 km)
S: Short River (10-100 km)

**: Free flowing rivers (CSI >= 95% over the entire length of river

Good connectivity status (CSI >= 95% over parts of river
Impacted (CSI < 95%)
Loss of free-flowing status due to future dam building

***: 1 : Local
2: Regional
3: Global
4: Climate change studies
5: Methodology only

****: Tier 1: Priority basin that should be processed first (less anthropization and/or data availability)
Tier 2: Others

*****:

Zone A: Tropical or equatorial
Zone B: Arid or dry zone
Zone C: Warm/Mild temperature zone
Zone D: Continental zone
Zone E: Polar zone

2.2 Description / characterisation

This section provides a brief description and main characteristics of each selected basin.

2.2.1 Amazon

The Amazon River basin (Fig. 2) occupies an area of around 6.2 million km² from the Andes mountains (west part) to the Atlantic Ocean (east part). It extends through Brazil (63%), Peru (17%), Bolivia (11%), Colombia (5,8%), Ecuador (2,2%), Venezuela (0,7%), and Guyana (0,2%) (ANA, 2017). It is, and by far the river with the highest mean annual discharge in the world. According to the GRDC database, its mean annual discharge at its outlet is equal to the sum of the mean annual discharges of the 6 following exorheic rivers with the highest discharge in the world (i.e. Congo, Orinoco, Yangtze, Ganges/Brahmaputra, Yenisei, Mississippi, and Lena).

The main air temperature varies between 24°C and 26°C (IMMET, 1992) whereas the annual average rainfall is between 1000 and 3000 mm across most of the basin with peak values around 4000 mm (north-western part) and minimum value around 100 mm (southwestern part; Heerspink et al., 2020). In the southern part of the basin, the rainy season extends from November to March and in the northern part, the rainy season extends from May to October (Nobre et al., 2009). The far north and north-western regions of the basin remain wet throughout most months of the year (Espinoza Villar et al., 2009)

The Amazon River and its tributaries constitute the largest source of fresh water on land (Tourian et al., 2018). The river basin releases approximately 209 000 m³/s (or 20% of the global discharge) of fresh water to the ocean (Marengo, 2005). The major tributaries come from the Andes (Seng Japura, and Madeira rivers), in the sub Andean trough (e.g. Purus rivers), in the Guyana Shield (e.g. Negro rivers) or drain the Brazilian Shield (e.g. Tapajós). According to Latrubesse et al. (2005,

2017), 20 of the 34 largest tropical rivers are Amazonian tributaries and four of the 10 largest rivers in the world are in the Amazon Basin (the Amazonas, Negro, Madeira, and Japurá rivers).

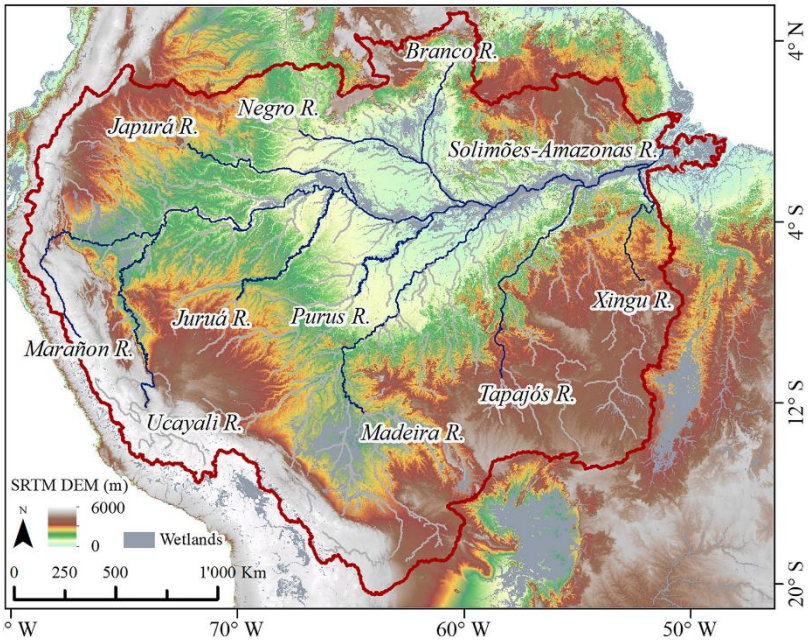

Figure 2. The Amazon River basin (limits indicated by the red line) with its main hydrological features: small and large rivers (in grey and blue lines respectively, the names of main tributaries are provided) and wetlands (grey areas). The DEM from SRTM is represented underneath. Adapted from Fassoni-Andrade et al., 2021.

2.2.2 Chad

The Chad basin is located in the centre of the African Sahel and is one of the most important endoreic watersheds in the Sahel due to the dramatic decrease of water level and extent during the last decades and also the largest one in the world Gao et al., 2011). It extends through multiple African country where the main part in Chad and Central African Republic.

The mean annual precipitation decreases rapidly from the southern part to the northern part with respectively values from more than 1000 mm/year to less than 100 mm/year (Niel et al., 2005). The outlet of this endoreic basin: Chad lake, was reduced to about 20% (427 000 km²) of the initial condition since 1964 (Lemoalle et al., 2014) and continued to decrease till it today divided into a dry and hydrologically disconnected northern part and an active southern part (Mahamat et al., 2021)

For this study, only the southern part of the basin will be considered as it corresponds to more than 90% of the inflow to Lake Chad (Fig. 3). The lake is predominantly fed by two main perennial rivers: the Chari and the Logone. Although the south-eastern part includes about 300 000 km² of floodplains which constitute the 8th largest area of wetlands in the world (Niel et al., 2005).

The Lake Chad occupies a predominant position for locals and economy. It provides freshwater, fish and also aids pastoral and agricultural land for a large population.

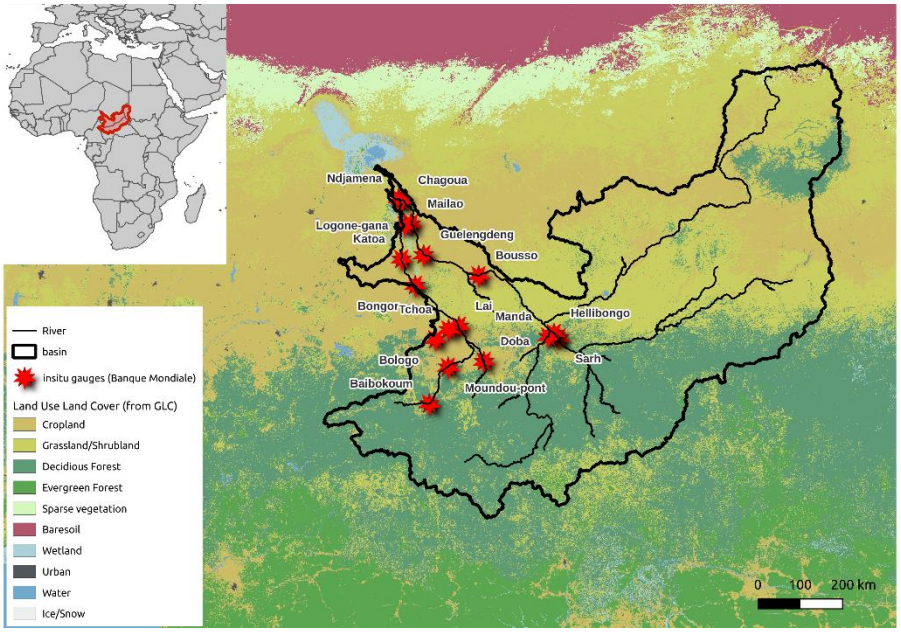

Figure 3. South-eastern part of the Chad River watershed with land cover (GLC)

2.2.3 Colville

The Colville basin drains the North Slope of Alaska. It drains an area of 53 600 km² (Fig 4). The area has arctic maritime climate with cold summers (15 °C in August) and winters, which last for about 8 months with temperatures goes down to -50 °C. Precipitation amount varies from 200 to 300 mm in foothills. About 50% of precipitation fall as snow. The area is located in continuous permafrost zone. As the result, streamflow in the Colville River ceases in winter months because of freezing of full ground profile. Thus, the hydrologic year for the Colville averages only about 4 months in contrast to that of the Mackenzie River, which spans the entire year (Walker HJ, Hudson, 2003). Streamflow in the Colville R. usually begins in early May in the upper reaches of its basin, and slightly later in its lower reaches. Spring, from a hydrologic standpoint, is dominated by flooding. After spring flooding, the summer season lasts for about 3 months. The river represents flow conditions typical for medium and small size rivers fully located in continues permafrost zone. Several studies noted an increase in air temperature and snow depth in the basin which already resulted in increase in permafrost temperature and bank erosion rate [Payne et al., 2018]. Historical observation of the river discharge also demonstrated a flow increase.

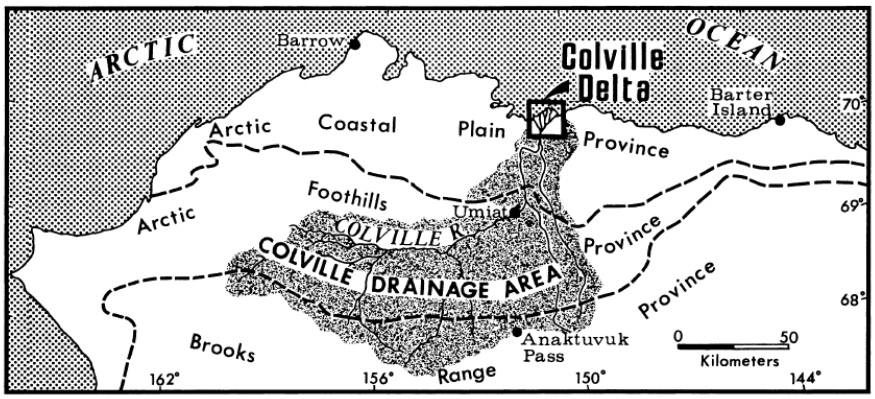

Figure 4. Colville River watershed (Cited from Walker et al., 2003)

2.2.4 Congo

The Congo River Basin (CRB) is the second-largest basin on earth and drains more than 3.7 million km² (Fig. 5). Despite this major contribution to the word's freshwater cycle, its hydrological behaviour is not fully understood yet. The Congo's mean annual flow is around 41 000 m³/s (Laraque, 2013). This mean flow is remarkably stable (Spencer et al., 2016) which make it an interesting singularity. Despite its critical importance to local, regional, and global water (Hastenrath, 1985) and carbon cycles (Dargie et al., 2017), the CRB has not received as much attention as the Amazon or other large river basins (Alsdorf, 2016). In the CRB, most people rely on local resources, which are strongly impacted by climate change and water availability (Youssoufa Bele, 2013). Hence, the undergoing climate changes (Nguimalet, 2017; Nguimalet & Orange, 2019; Samba & Nganga, 2012) are expected to have severe implications on the populations (Aloysius and Sayer, 2017; Nguimalet & Orange, 2013).

The mean temperature is approximately 25 °C whereas the mean annual rainfall varies between 2000 mm/year in the central parts of the basin, and 1000 mm/year both northward and southward. The annual potential evapotranspiration is around 1000 mm/year and slightly varies across the basin.

The basin is characterized by four main drainage systems (Ubangi River in the northeast, Sangha River in the north west, Kasai River in the south west and Lualaba River in the south east) that converge to form the main Congo River (see Fig.5).

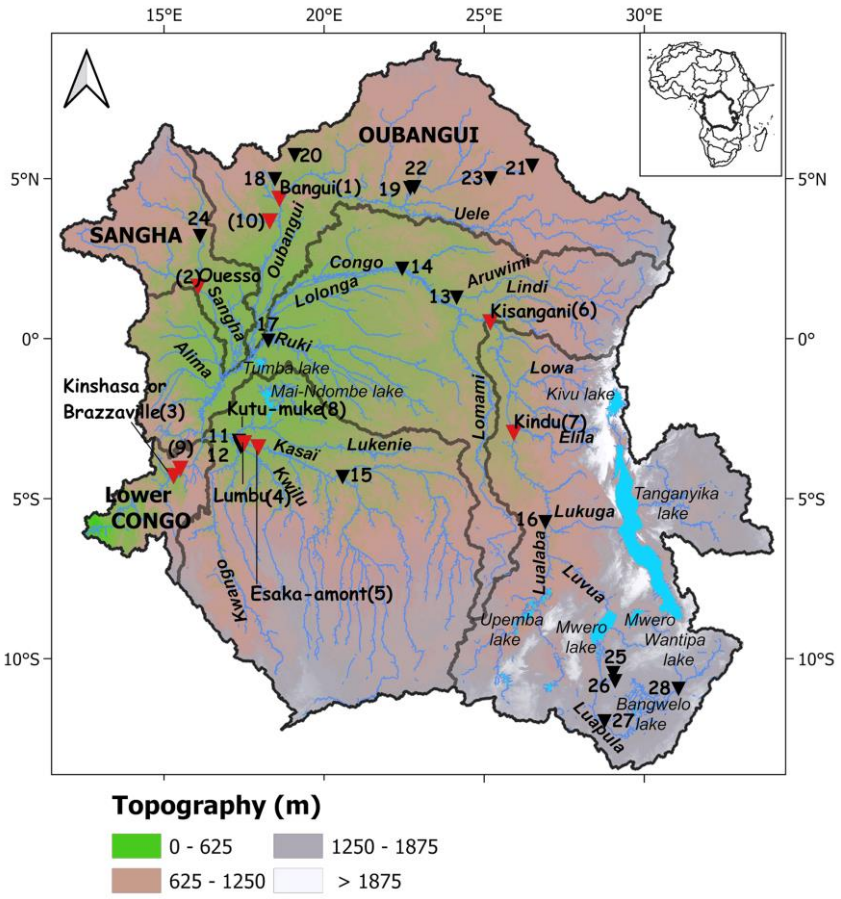

Figure 5. Topography of the Congo River basin derived from the MERIT digital elevation model. Red and black triangles represent, respectively, the gauge stations with current (> 1994) and historical observations (from Kitambo et al., 2022).

2.2.5 Danube

The Danube is the second largest river in Europe (Fig. 6), with a total length of 2826 km and a basin area of about 801 000 km². With 11 major tributaries, the Danube basin comprises parts of 19 countries (Germany, Austria, Switzerland, Italy, Slovenia, Slovakia, Hungary, Romania, Croatia, Serbia, Montenegro, Bulgaria, Moldova, Poland, Czech Republic, Bosnia-Herzegovina, Albania, FYR of Macedonia) and is hence the most international river basin in the world.

The Danube basin includes glacier-covered mountains in the Alps, the mid-mountains mostly covered with dense forests, karst regions with little vegetation, uplands, lowlands and wide plains. It flows from East to West into the Black Sea within a wide delta shared by Romania and Ukraine. It is the 23rd exoreic basin with the highest annual discharge, according to GRDC database. It has been chosen because it is a mid-latitude basin in Europe, where some gages data are available, at least in the upper part of the basin.

Fig 6: The Danube River basin and its major tributaries (from Stagl & Hattermann, 2016)

2.2.6 Ganga-Brahmaputra

The drainage area of the Ganges basin is about 1.07 million km². It is shared among China, India, Nepal and Bangladesh. The Brahmaputra has a drainage area of about 574 000 km² and is shared among China, India, Bhutan and Bangladesh. The Brahmaputra can be considered unregulated with no major hydraulic structures, whereas the Ganges is highly regulated with around 35 dams and diversion points in India and Nepal. Both the Ganges and Brahmaputra rivers originate in the Himalaya mountains and join in Bangladesh before reaching the Bay of Bengal (Fig. 7).

The combined Ganges/Brahmaputra/Meghna basin is the third biggest discharge river basin in the world, according to the GRDC database. It is monsoon-driven and has been chosen for its size and its importance in South-Asia. But of course, discharge in the upper part of each basin is driven by glacier and snow thawing. Precipitation is quite heterogeneous on the basin (Fig. 7). On the Ganges, the maximum precipitation occurs in July/September time span and the mean monthly rainfall is in between 250 and 300 mm/month over 1975-2004 (Jian et al., 2009). But on some part of the lower Brahmaputra River, annual precipitation could be above 2000 mm.

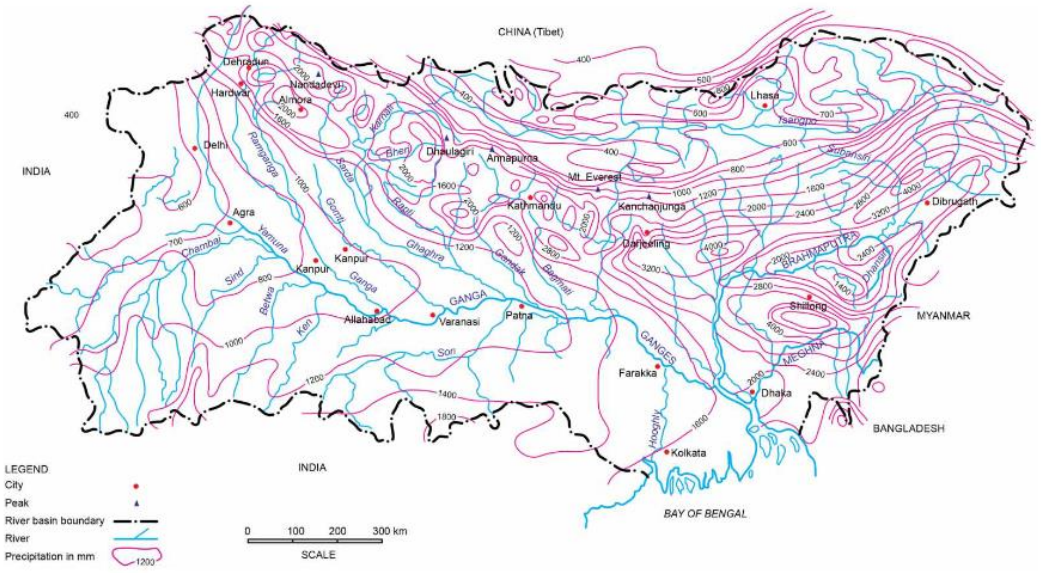

Figure 7. Annual precipitation in the GBM region. Adapted from Bandyopadhyay (1995)

2.2.7 Garonne

The Garonne basin (Fig. 8) drainage area at the Gironde estuary is around 56 000 km². The mean annual discharge near its outlet is around 600 m³/s It is the 120th largest river in the world by its annual discharge. The Garonne River has a pluvio-nival regime, with a low flow period from July to October, and high flow period from December to April. It is a highly anthropized basin, as 70% of the total water uptake during low flow period comes from agricultural activities.

This basin has been chosen, as a test basin: it is a well gaged basin and it is a small basin with some locations with drainage area <50 000km². The river width near Tonneins and Marmande is around 150m.

Garonne hydrology has experienced some low flow periods longer and more important in the last years compared to previous decades. A 25/30years-return period floods occurred in June 2000 and January 2022 in the middle basin.

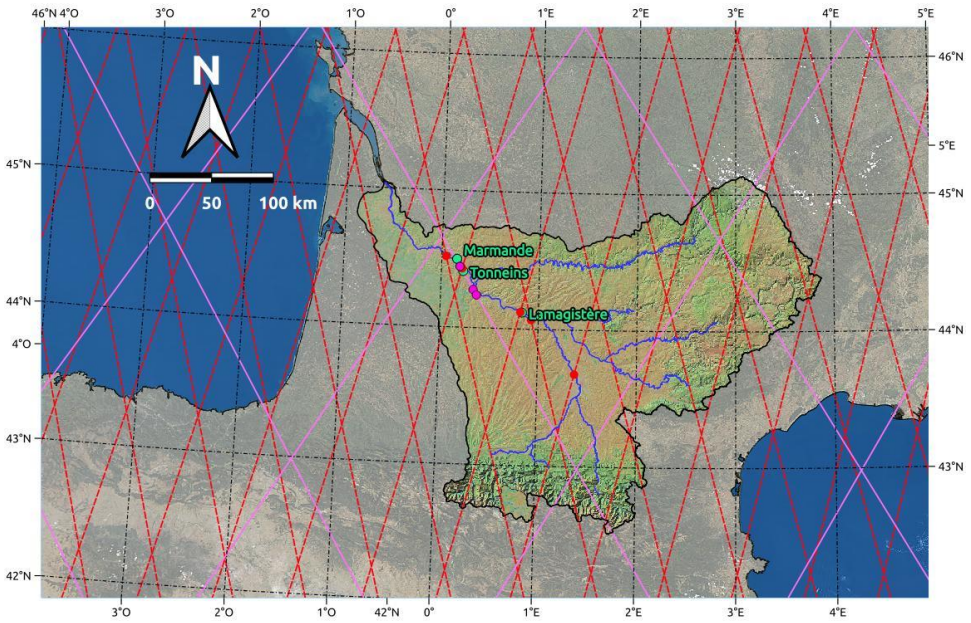

Figure 8. Garonne basin with available discharge and WSE in situ gages (green dots) and WSE altimetry from Jason-2/3 (magenta dots, magenta lines corresponding to Jason tracks) and Envisat (red dots, red dashed lines corresponding to Envisat tracks). Adapted from Biancamaria et al. (2017)

2.2.8 Indus

The Indus River (Fig. 9) is large transboundary basin, crossing China, India, Pakistan and Afghanistan. Its total length of about 2800 km, and its total drainage area is around 1 million km^2 (Ali, 2013). The Indus River source is in the Tibetan Plateau (China) and it discharges to the Arabian Sea. The Indus Basin climate is semi-arid (note that the upper part of the basin is also glacier-fed and snowmelt-fed) and monsoon-driven (mainly in Summer).

The basin is heavily anthropized in Pakistan, with 21 dams, 12 inter-river canals, about 56 000 km of canals, and about 110 000 km of water courses (Ali, 2013). 14 million hectares of land in Pakistan relies on water from the Indus for irrigation. Because of alle these infrastructures, the Indus River discharge is decreasing downstream in the lower part of the basin. Therefore, estimating discharge at the basin outlet from satellite data can be very challenging.

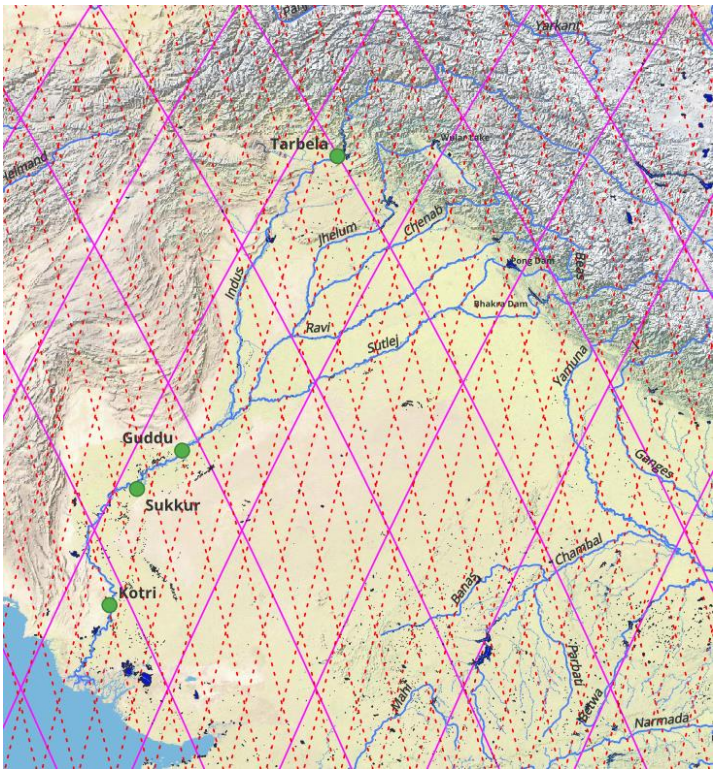

Figure 9. Dam locations for which upstream and downstream in situ discharge is available during the monsoon period in the online FFC annual flood reports. Magenta lines correspond to Jason-series ground tracks and red dotted lines correspond to ERS/Envisat/Saral ground tracks.

2.2.9 Irrawaddy

The Irrawaddy basin drains 411 000 km^2 and is shared among Myanmar (most part), China, and India (Li et al., 2021). The source of the Irrawaddy is located in the Tibetan and Naga mountains. The Irrawaddy River flows from north to south (Fig. 10) and empties into the Andaman Sea at Yangoon. The central Irrawaddy basin consists of large arid plains with relatively low precipitation and distinct dry and rainy seasons in contrast to the lower plains, which experience a tropical monsoon climate and abundant precipitation (Li et al., 2021). It is the 17th river with the biggest annual discharge in the world, according to GRDC database.

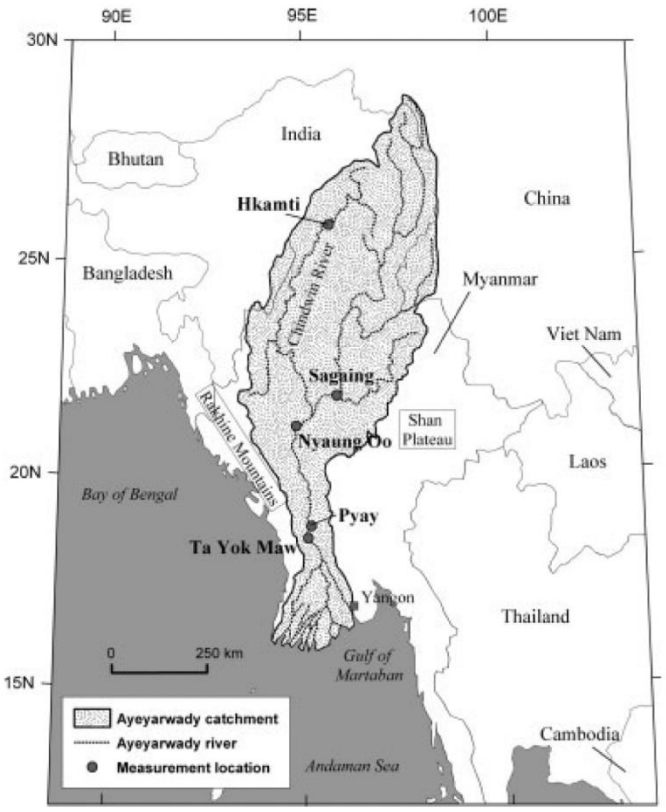

Figure 10: The catchment of the Ayeyarwady River (from Furuichi et al., 2009)

2.2.10 Lena

The Lena River is located in Central Siberia. It originates on the western slopes of mountains bordering Lake Baikal from the West and flows into the Arctic Ocean through the Laptev Sea. The Lena River drains an area of 2.43 million km². The most part of flow volume is generated in the upper and middle reaches. 1310 km from the delta, the Lena River receives water from its biggest tributary, the Aldan River, and 1100 km the Viluy River, later provides the last big water input (Fig. 11).

The climate in the region is strongly continental. The mean annual temperature is −10 °C. In winter, the temperature decreases below -50 °C. For eight months of the year (from October until May), the watershed is covered by snow. The mean annual atmospheric precipitation ranges from 700 to 800 mm in upper reaches (orographic effect) to less than 250 mm in the middle and lower reaches. The basin lies in the permafrost zone. In the upper reaches the permafrost is relatively warm (temperature of the frozen soils is close to 0 °C). During last two decades changes in atmospheric circulation resulted in changes in temperature and precipitation regime. These led to rapid degradation of permafrost and abrupt changes in surface water balance in the central part of the basin. On the Viluy River the Viluy reservoir was constructed in 1965-67. The regulation capacity of the reservoir is of 22.4 km³. The Lena River upstream from the Aldan tributary is prone to inundations. The inundations affect fragile local agriculture with unique practices for permafrost zone.

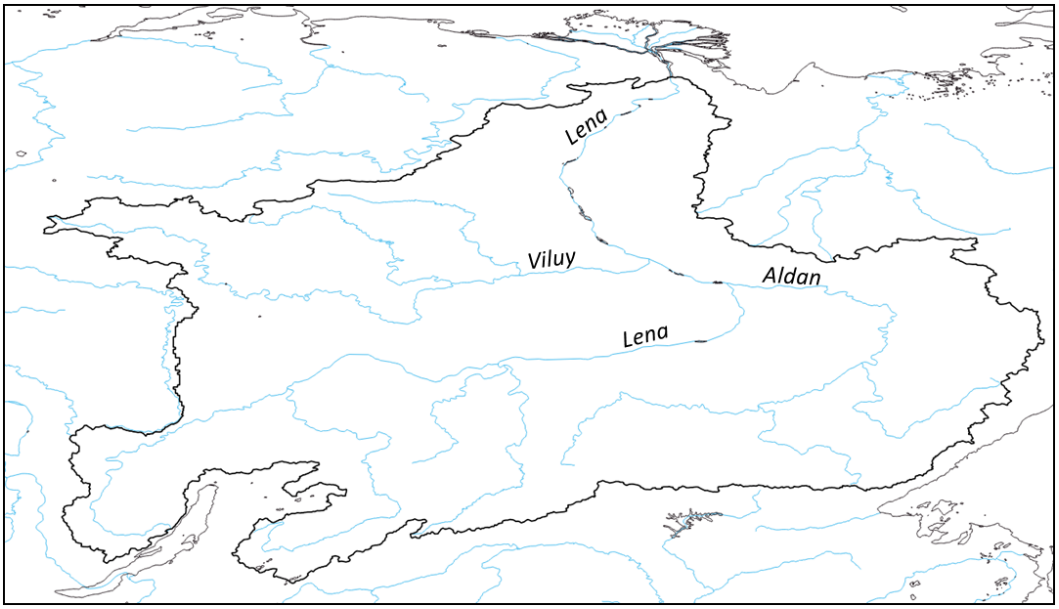

Figure 11. Lena River watershed

2.2.11 Limpopo

The Limpopo Basin (Fig. 12) is located in southern Africa and shared between Botswana, South Africa, Zimbabwe and Mozambique, where it flows into the Indian Ocean and covers an area of approximately 400 000 km². The area consists of gently undulating to highly variable altitude, with lowest and highest points at about 850 and 1400 m above sea level

The rainy season is controlled by the Inter Tropical Convergence Zone (ITCZ) and is usually lasts from October to March. The average annual rainfall ranges from 250 to 1050 mm/year with 530 mm on average per year, but with high inter-annual variability which makes drought a common natural hazard. Rainfall occurs over a limited period of time, and often a large portion of the annual rainfall can fall in a small number of events (De Groen & Savenije, 2006).

Mean annual runoff is approximately 4.55 million m³/year (outlet) and the main rainy season runoff lasts from December to May. Many of the streamflow time series are heavily affected by water use and management especially the dams (FAO, 2004).

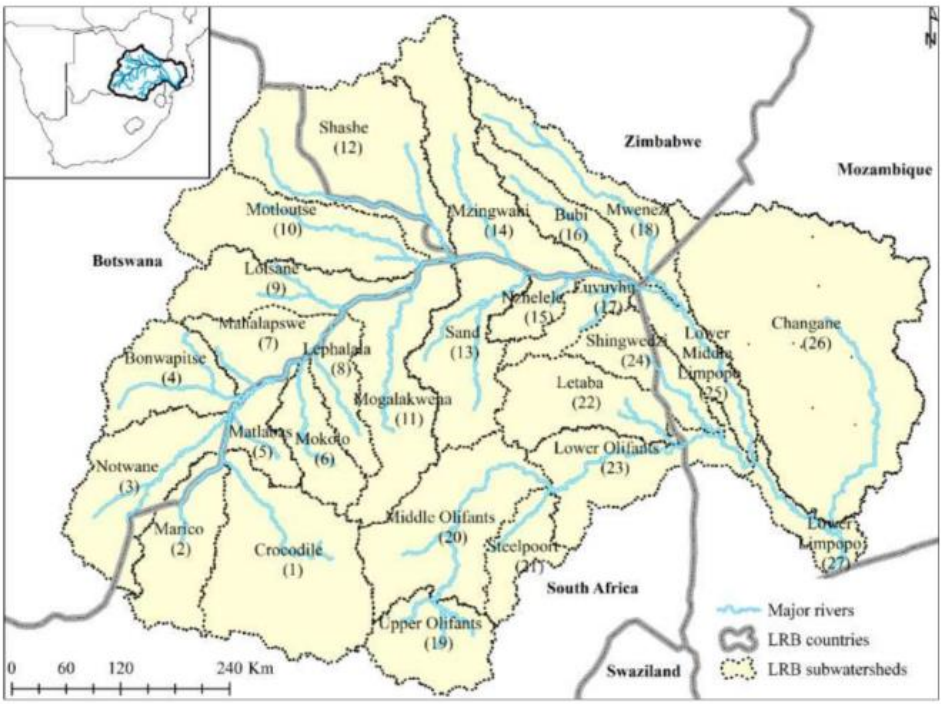

Fiugure 12: The Limpopo River Basin in Southern Africa and its twenty-seven designated subbasins, herein referred to as watersheds (from Mosase & Ahiablame, 2018).

2.2.12 Mackenzie

The Mackenzie is the largest northward flowing river in North America (Fig. 13). It drains an area of 1.8 million km², about 1/5 of the total land area of Canada (Yang et al., 2015). Its headwaters collect a vast system of rivers which flow into Great Slave Lake, from which the Mackenzie River proper flows in a north-westerly direction for about 1600 km before discharging through the Mackenzie Delta into the Beaufort Sea. The freshwater contribution is about 325 km³/year, or approximately 7% of the annual inflow to the Arctic Ocean as a whole. Permafrost and wetland cover approximately 75% and 49% of the basin (Yang et al., 2015).

The basin has several climatic regions, including cold temperate, mountain, subarctic, and arctic zones. Mean annual temperatures vary from around −10 °C to 4 °C, and annual precipitation ranges from more than 1000 mm in the southwest to about 200 mm along the arctic coast, average about 410 mm per year (Woo and Thorne, 2003, Woo and Thorne, 2014).

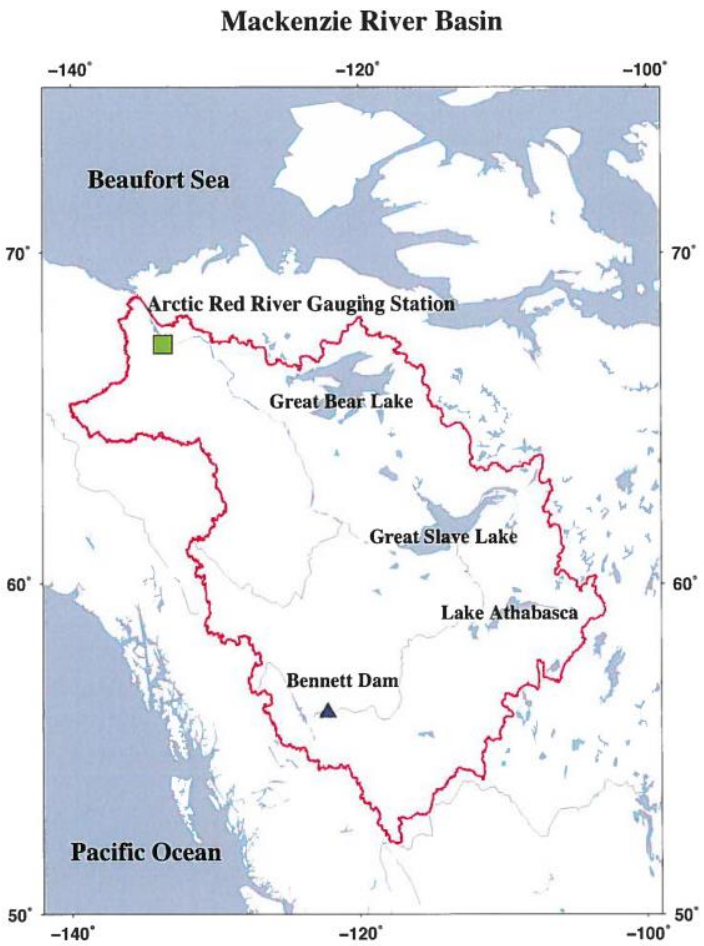

Figure 13. Mackenzie River basin (cited from Yang et al., 2015)

There are many lakes in the basin. The three large ones are Lake Athabasca, Great Slave, and Great Bear lakes, with surface areas of 79 120, 28 600 and 31 300 km² respectively. These lakes provide natural flow regulation to the system. One large reservoir (the Williston Lake reservoir, surface area is around 18 000 km²) has been built in the upper Peace River. The reservoir may substantially influence the water level fluctuations in Great Slave Lake; but did not significantly affect the flow conditions at the lower Mackenzie (Peters and Prowse, 2001, Woo and Thorne, 2003). However, a work by Woo and Thorne (2014) reports that the release of water from the reservoir at the Peace River provides 40–60% of the winter flow of the Mackenzie River. This result is similar to the observed seasonal regulation effect found for the Ob River.

2.2.13 Maroni

The Maroni River basin is more than 60 000 km² wide and is located in South America. Its principal river, the Maroni, forms the frontier between France (French Guyana) and Suriname. Since the basin is in deep Amazonian Forest, the Maroni River is one of the main vectors of wellness and goods for populations living, in their huge majority, in the coastal or riverine area. At the same time, it also a very porous frontier and drains a large number of illegal workers crossing the border in

order to find spots for illegal mining activities. Such activities have a strong impact on water quality and sediment fluxes (Gallay et al., 2018; Do et al., 2020).

Its hydrological regime is characterized by a mean discharge of about 1700 m^3/s, and classified as Af according to Koppen classification. From upstream to downstream, it presents several breaks in its bathymetry that turns navigation uneasy during low or extreme high flows. Fig. 14 provides the limits of the basin together with the main sub-basins and the principal river network.

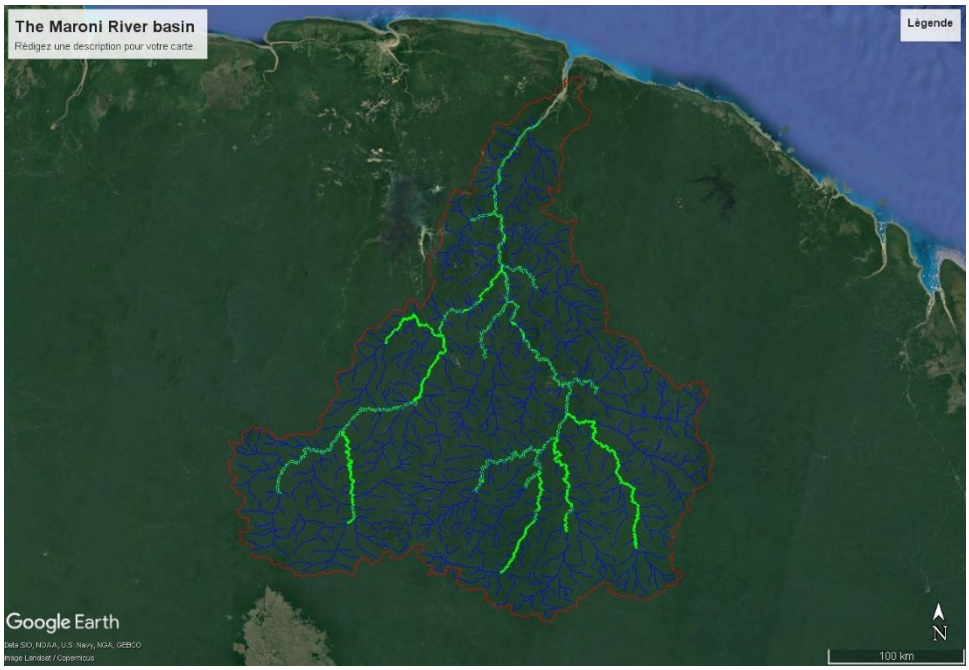

Fig. 14: Contour of the Maroni River basin (red line) with the main river reaches (green) and more extended river network (blue).

In the Maroni River basin, the in-situ monitoring network, operated by SCHAPI (see 3.1.8) is composed of seven (7) in situ gages, including one recently installed on the left tributary coming from Suriname, the Tapanahoni River. However consequent, this sampling is not always sufficient for purposes such as real-time monitoring (because of the Amazon dense forest, many connections loss occur) or long-term and climate studies (only part of the basin was monitored in the past, continuity in observation are not easy to ensure, etc.). Yet, some stations provide long observation of water level and discharges. As the basin and the entire territory is now facing climate change effects and is accessible since located in France, it is a good candidate for application and validation of methodologies for discharges estimates from space.

2.2.14 Mississippi

It is a mid-latitude basin (Fig. 15) and it is the largest one in the US, with a drainage area around 3.1 million km^2 (40% of the contiguous USA). It is the 7th exoreic basins on earth with the largest discharge, according to GRDC data. Its mean annual flow at Vicksburg is around 17 000 m^3/s. It provides water supply to nearly 18 million people and corresponds to 25% of the USA' hydropower (Lewis et al., 2023). In addition to dams and irrigation intakes, many flood protection infrastructures on the Mississippi river networks have been built since the major flood of 1927 (Lewis et al., 2023).

Milly and Dunne (2001) showed that over the basin, a precipitation increase during the second part of the 20th century impacted runoff, evaporation, surface net radiation, and evaporation. According

to Lewis et al. (2023), the 100-year return period discharge at Vicksburg could increase by 8% into the future period, because noteworthy of climate change among other things

Thanks to the important gages network maintained by the United States Geological Survey (USGS), the Mississippi basin is one of the best observed watersheds in the world in term of river discharge and water level (see section 3.2.14). This basin is therefore a perfect basin to validate uncertainties on discharge and WSE derived from different methodologies.

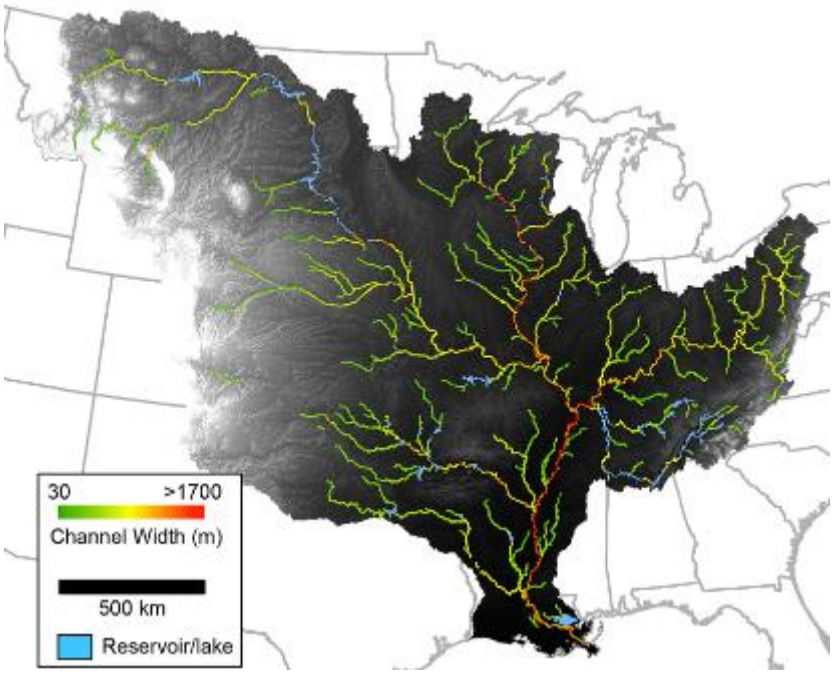

Figure 15. Mississippi River derived from Landsat images map (shown with USGS HydroSHEDS DEM in background) from Miller et al. (2014)

2.2.15 Niger

The Niger River is West Africa's largest river, with more than 100 million inhabitants within the 2.1 million km² watershed area. The river basin extends into nine countries and spans several climate regions, from humid tropical to desert (Fig 16). The river is an important natural resource, often key for livelihoods, especially in Mali and Niger. Substantial rainfall decreases in the Sahel have led to major disasters such as the droughts and famines of the 1970s and 1980s (Mahé et al., 2013). More recently, floods are a growing concern taking lives and damaging infrastructure; and resulting in personal tragedies, substantial repair costs and disruption of transportation. Increasing flooding in recent years (e.g. in 2008 , 2016 and 2020) can partly be attributed to climate variability but also to land use changes and land cover modification due to major drought (Gal et al., 2017). The region has been designated as a particularly sensitive area for potential future climate change (Diallo et al., 2016). Better understanding of historical river discharge and more especially, peak flows, could contribute to improved infrastructure design, and operational flood forecasts could facilitate emergency response and thereby increase societal resilience to future floods in the region.

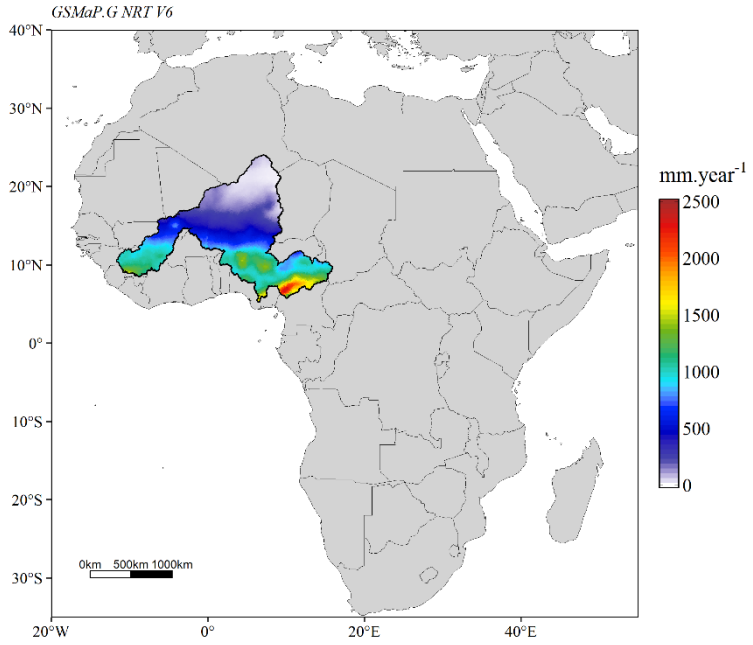

Figure 16. Niger basin with mean annual accumulated precipitation (2002-2022) from GSMaP NRT V6 - Courtesy of R. Oliviera

2.2.16 Ob

The Ob' has the largest watershed of all Arctic rivers (2.98 million km²) and is the third largest contributors of freshwater to the Arctic Ocean (mean annual flow of 402 km³/year, Kouraev et al., 2004) after the Yenisey and Lena rivers (Fig. 17). The Ob' length is of 3 680 km from the confluence of Biya and Katun' rivers in the Altay Mountain region to the Ob' bay in the Kara sea. A large part of the watershed is located within the West Siberian plain and the flat relief significantly affects the hydrographical network. The Ob' of the West Siberian plain is also characterised by large flooded areas, frequently described as the biggest world swamps. The region is abundant with lakes (over 450 000), mainly small lakes with surface area less than 1 km² and depths of 2–5 m. The watershed extents from 47.8°N to 68.8°N. The natural conditions vary from step-forest on the south to tundra on the north. At ~61°N the patchy permafrost appears; its coverage progressively increases toward the north. The diversity of conditions results in progressive gradual melting of snow during the spring and in a smooth temporal variability of the discharge during the spring flood. The Ob' discharge starts to increase in April, when the flood wave begins to break the ice cover, and reaches maximal values in May–June. During this time, large areas of the Ob' basin are flooded. The discharge then gradually decreases until July–August, and in September–October an autumn low level period is observed. About 75–80% of the annual flow is observed during the open water period before the river gets covered by ice until the next spring. In the Ob R. basin there are two reservoirs located in upper reaches : Novossibirskoe (Ob River) and Bukhtarminskoe (Irtysh River). Novossibirskoe was constructed in 1957 and has 8.8 km³ of storage capacity and 4.4 km³ of regulation capacity. The reservoir is mostly used for seasonal regulation of flow. Bukhtarminskoe reservoir was filled up in 1966. Its full volume is of 50 km³ and regulation capacity is of 31 km³. Due to this big regulation capacity, the reservoir is capable of regulating inter-annual flow. In lower reaches of the Ob River, the seasonal flow regulation could be seen only in winter discharges. The signal of spring flow interception by reservoirs is hidden by high spring water contribution of big tributaries.

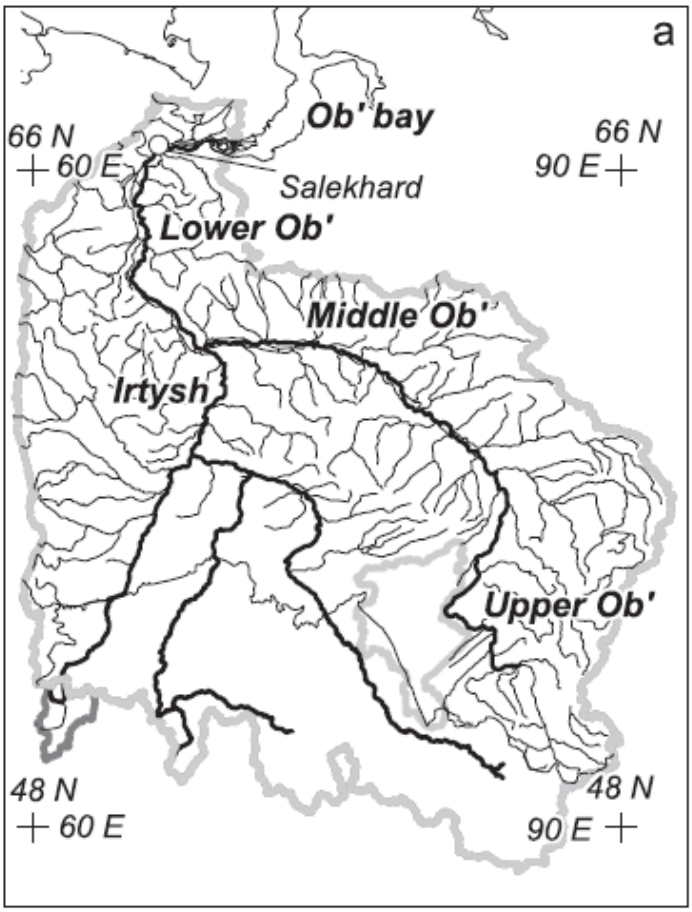

Figure 17. Ob River basin and its main hydrographic network.

2.2.17 Po

Located in northern Italy, the Po River flows from West to East for 652 km through the Po Valley, making it the longest and widest river in Italy. The morphology of the river is that of a single branch, with the main river width ranging from 200 m up to almost 500 m, while the lateral floodplains are delimited by a system of large levees and can reach an extent of 5 km (Montanari, 2012). The embanked floodplains are usually used for agricultural purposes and some areas are protected from frequent flooding by a system of smaller dikes. The Po basin covers an area of about 74,000 km^2 and includes almost the entire territory of four regions (Valle d'Aosta, Piedmont, Lombardy and Emilia Romagna, as well as a part of Veneto with regard to the delta in the province of Rovigo), as well as small parts of neighboring regions (Liguria, Tuscany and the Autonomous Province of Trento) and about 150 km^2 of Swiss territory (Figure 18).

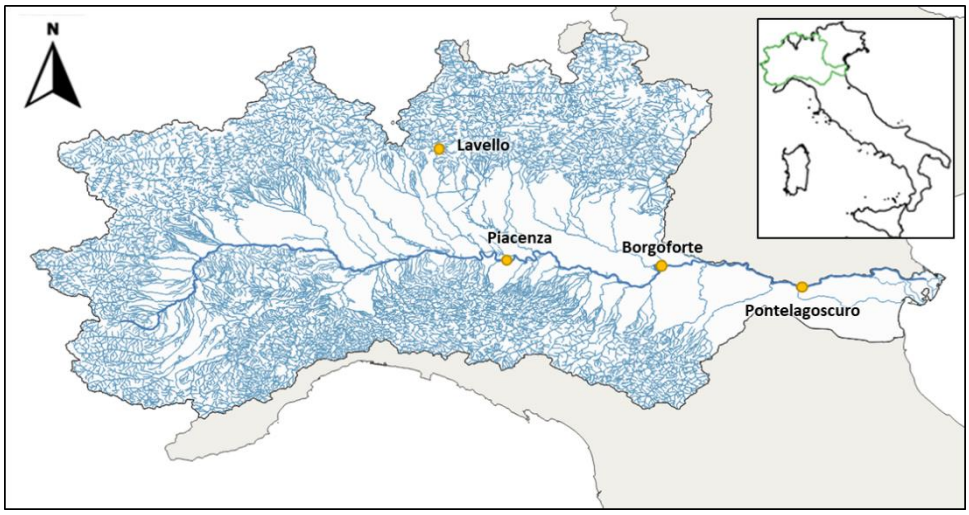

Figure 18. Po River basin and its main hydrographic network. The stations selected for the projects are also shown.

2.2.18 Zambezi

The Zambezi River Basin is located in the semi-arid zone of southern Africa and is the fourth largest river basin in Africa, with a total drainage area of approximately 1.3 million km² (Fig. 19). The mainstream, with a total length of 3000 km, originates in the Kalene Hills in northwest Zambia at an altitude of 1500 m and flows eastwards to the Indian Ocean.

The river is divided into three parts/watersheds: the Upper Zambezi with gentle slope and large floodplains, 2) the Middle Zambezi with an important evaporation and lot of floodplains, and 3) the Lower Zambezi characterized by steep slopes mainly in the upstream. These watersheds cover together more than one third of the whole Zambezi watershed and contribute more than one half of the total runoff. The main

The climate of the basin is largely controlled by the Inter-Tropical Convergence Zone (ITCZ). Rainfall occurs predominantly during the summer (November to March), whereas the winter months (April to October) are usually dry (Beyer et al., 2016). The total amount of rainfall over the basin is on average around between 990 and 1000 mm/year and varying from 1200 mm/year in the northern parts to 700 mm/year in the southern parts of the basin with an average annual potential evaporation between 1000 and 2000 mm (World Bank, 2010). However, rainfall is characterized by considerable spatial and temporal variation throughout the basin. Droughts and floods are common natural hazards.

Throughout the basin runoff arises in response to complex interactions between surface flow and saturated and unsaturated subsurface flow. The natural flow regime of the Zambezi River reflected the rainfall and was characterized by high seasonal and annual variability. The total discharge of the river is estimated around 4.1 m³/s which equate to 95 mm over the entire basin (i.e., a runoff coefficient of 9.6%).

Due to the absence of large dams, the Upper Zambezi remains the most natural portion of the river. Further downstream, the flow is regulated by a number of large dams (Nones et al., 2013) leading to a flow increase during the dry season and a decrease and delay of peak flows during the flood season.

Figure 19 : Zambezi waterhsed and its main rivers (respectively in black and blue). Big lakes are identified (blue areas) and swamps and wetlands also (violet areas). Countries limits are in red line. Source: Zambezi River Authority: http://www.zambezira.org/media-centre/maps/zambezi-river-basin.

3 Data availability

3.1 Databases

The in-situ discharge databases are available thanks to two main worldwide collections of metadata:

- The Global Runoff Data Base (GRDB) maintained by the Global Runoff Data Centre (GRDC) with daily and/or monthly discharge time series available over more than 900 stations worldwide (see section 3.1.1)
- The GSIM (Global Streamflow Indices and Metadata Archive) is a worldwide collection of metadata and indices derived from more than 35 000 daily streamflow time series (see section 3.1.2).

Besides these global databases, there are several continental (like ADHI, see section 3.1.3), or national/regional networks (see sections 3.1.4 to 3.1.9). The last section corresponds to satellite databases that will be used within the project.

3.1.1 GRDB

The Global Runoff Data Base (GRDB) maintained by the Global Runoff Data Centre has been the primary dataset used in large-scale hydrological studies, with more than 9000 stations available to the research community (GRDC, 2015). The Global Runoff Data Centre (GRDC) is an international archive of data up to 200 years old and fosters multinational and global long-term hydrological studies. Originally established three decades ago, the aim of the GRDC is to help earth scientists analyse global climate trends and assess environmental impacts and risks. https://www.bafg.de/GRDC/

Even if numerous countries have databases of acceptable quality, data supply remains resource intensive and the GRDB remains sparse in some regions. For example, the latest catalogue of the GRDB database (end of 2017) shows that out of more than 7000 daily time series, only 10% are available over South America and another 10% over Asia. Moreover, many stations in regions such as Asia and Russia have not been updated for many years and are missing otherwise available data at the end of their records

3.1.2 GSIM

The GSIM (Global Streamflow Indices and Metadata Archive) is a worldwide collection of metadata and indices derived from more than 35 000 daily streamflow time series (Do et al., 2018; Gudmundsson et al., 2018). The GSIM yearly/seasonal/monthly time series can be downloaded at PANGEA data repository (https://doi.pangaea.de/10.1594/PANGAEA.887470), see Annex A for more detailed information.

The GSIM project has been initiated in order to address the demand for a global streamflow database. The approach of this project is not to collect high-quality data from referenced hydrological networks, which have been conducted in other studies to support research that requires assumptions regarding the minimum impact of human interference on streamflow, such as the investigation of climate change implication for changes in extreme events. Instead, the activities of the GSIM project have been to collate publicly available data, apply basic consistency to the formatting, and establish a standardized set of metadata.

3.1.3 ADHI

The ADHI (African Database of Hydrometric Indices; Tramblay et al., 2021) is a collection of stations from the Global Runoff Data Center (GRDC) and the SIEREM database (Boyer et al., 2006; Dieulin et al., 2019). It contains daily/monthly discharge time series for ~1500, covering at least 10 years over the period 1950-2018 (time series covers in average 19 years). The monthly time series can be downloaded on the following repository: https://doi.org/10.23708/LXGXQ9.

3.1.4 ANA

The Brazilian National Water Agency (ANA) provides a database with all the information collected by Brazil's hydrometeorological network. Streamflow data and associated metadata were made publicly available by Brazil's national water regulations, and have been used extensively to monitor critical events, such as floods and droughts. Individual time series and their associated metadata can be viewed or downloaded at http://hidroweb.ana.gov.br.

3.1.5 USGS

The U.S. Geological Survey's (USGS) supports the acquisition, processing, and long-term storage of water data. Water Data for the Nation serves as the publicly available portal to a geographically seamless set of much of the water data maintained within NWIS.

Nationally, USGS surface-water data includes more than 850,000 station years of time-series data that describe stream levels, streamflow (discharge), reservoir and lake levels, surface-water quality, and rainfall. The data are collected by automatic recorders and manual field measurements at installations across the Nation.

Data are collected by field personnel or relayed through telephones or satellites to offices where it is stored and processed. The data are processed automatically in near real time, and in many cases, current data are available online within minutes.

To download the streamflow data, you need to go to the National Water Information System (NWIS) web interfaceat the following link: http://waterdata.usgs.gov/nwis.

3.1.6 SIEREM

The Système d'Informations Environnementales sur les Ressources en Eau et leur Modélisation (SIEREM) started in 1999 with two simultaneous phases: data collection and the system analysis and design. The challenge was to build a system with both chronological data and spatialized information (such as soil, vegetation and DEM layers). HydroSciences Montpellier formed a team of engineers to start three tasks: collection of hydro-meteorological data and metadata, collection and building-up of geographical information, and the required data homogenization and integration into an environmental system built using a specific method of system analysis and design. The hydro-climatological data contained in SIEREM are the legacy of the former *Laboratoire d'Hydrologie* of the *Office de la recherche scientifique et technique outre-mer* (ORSTOM; now *Institut de Recherche pour le Développement*, IRD, France).

In addition to the daily data, the SIEREM database also contains instantaneous rainfall and discharge for hundreds of experimental small catchments mostly established in the 1950s and 1960s. Only monthly data are provided freely directly on the website: https://doi.org/10.23708/LXGXQ9.

3.1.7 AIPo

The Italian hydrological monitoring network is managed at regional level by different agencies. For the Po basin, the Agenzia Interregionale del Fiume Po (AIPo) is responsible for the coordination of the hydraulic activity, the management and improvement of river navigation infrastructures, environmental and river protection and the coordination of the flood service. For the management of extreme events, AIPo is involved in forecasting and monitoring. Specifically, the website of the agency (https://www.agenziapo.it/content/monitoraggio-idrografico-0) shows real-time and historical measurements that can be freely downloaded by any users.

Daily river discharge and water level data are available on the websites of the various regional agencies. For the main course of the river, it is sufficient to have access to data from the regions of Emilia Romagna and Lombardy. However, the platforms from which the data can be downloaded or the format of the data, are often not suitable for collecting data over many years or for use at an operational level.

3.1.8 SCHAPI

In France, in situ gages operated by regional public agencies (i.e. DREALs, Directions Régionales de l'Environnement, de l'Aménagement et du Logement) are collected by the SCHAPI (Service Central d'Hydrométéorologie et d'Appui à la Prévision des Inondations). SCHAPI releases these data publicly via the online “HydroPortail” national database (https://hydro.eaufrance.fr). These public agencies are responsible to observe and forecast floods, and to alert the population in case of dangerous events (https://www.vigicrues.gouv.fr/).

3.1.9 Bayerisches Landesamt für Umwelt

The Bayerisches Landesamt für Umwelt (i.e. Bavarian State Office for the Environment) is the agency responsible for environmental and nature protection, geology and water management in Bavaria. Especially, it provides online (https://www.gkd.bayern.de/en river water levels and discharge on the Danube at some locations within Bavaria (in the upper part of the Danube basin).

3.1.10 FFC

The FFC (Federal Flood Commission), linked to Pakistan’s ministry of water resources, regularly issues flood reports on last monsoon season. Those reports can be used as source of information on water levels and/or discharges in the locations issued in the reports. The reports can be found here: https://ffc.gov.pk/daily-flood-situation-reports/.

3.1.11 HyDAT

The HyDAT (Hydrometric DATa) Is the Canadian database for water levels and discharges. It provides both real-time information on hydrological situation of Canadian rivers and historical data that can be freely downloaded. The datasets can be found here: https://wateroffice.ec.gc.ca/.

3.1.12 Other national databases

In some basins, the data that will be available for this project comes from previous collaboration with national agencies (such as flood commissions, ministries of water, etc.) or data published in report or scientific articles. This kind of data is not part of an online database but are still available for the project. Also, we may obtain the authorization to use more data than initially expected. Data collected in public domain articles or reports does not have such constrains. For example, the

monthly average discharge at Pyay on the Irrawaddy River from 1966 to 1996 comes from Table 2 in Furuichi et al. (2009), who collected these data from the Department of Meteorology and Hydrology of Myanmar.

3.1.13 Satellite altimetry databases

The HydroWEB database (http://hydroweb.theia-land.fr), has been developed in LEGOS since 2003 to provide a database of water surface elevations (WSE) on lakes and rivers around the world based on satellite altimetry. Several thousand virtual stations are monitored and available in HydroWEB, in operational mode (real-time update) or in delayed mode. More than 150 lakes are also monitored, some in operational mode. In addition, changes in extent and volume are also measured for many of them. This service is hosted on the THEIA national cluster platform. It is operated by the company CLS in coordination with LEGOS, IRD and CNES. Some members of this CCI precursor project are directly involved in the HydroWEB database development and the project will have a full access to this database.

Other WSE from altimetry database exists and could be also used in this precursor project, even if no member of the project is involved in their development. These databases are (this list might not be exhaustive): Database for Hydrological Time Series of Inland Waters (DAHITI, http://dahiti.dgfi.tum.de), HydroSat (http://hydrosat.gis.uni-stuttgart.de/php/index.php) and Global River Radar Altimetry Time Series (GRAATS, https://doi.org/10.5067/PSGRA-SA2V2).

For WSE time series from some altimetry missions, that are not in these public WSE databases, will be derived using L2 Geophysical Data Records (GDR) products from different space agencies that are stored and reformatted by the CTOH (Center for Topographic studies of the Ocean and Hydrosphere; http://ctoh.legos.obs-mip.fr/) at LEGOS.

Fig. 20 presents a timeline of the altimetry missions that will be considered within this precursor project.

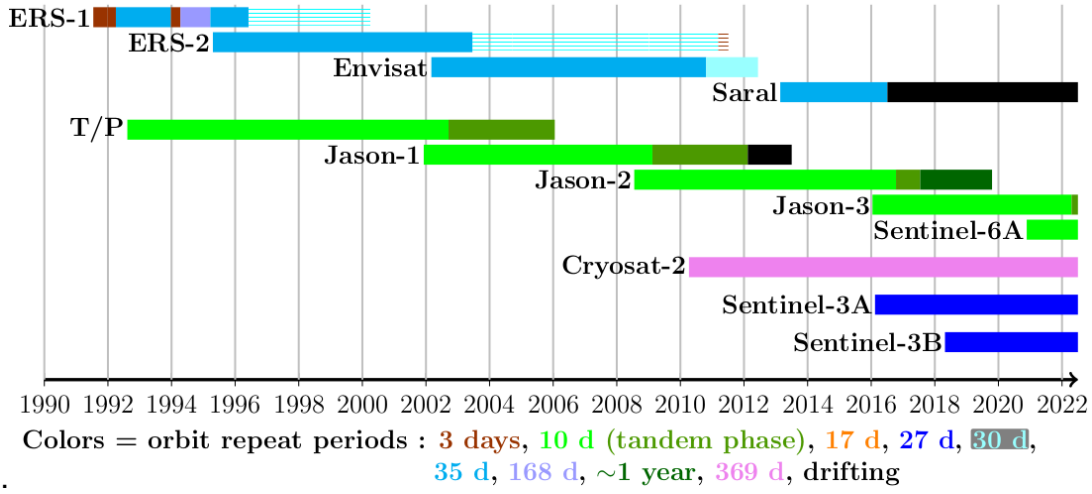

Figure 20. Timeline since 1990 of the altimetry missions that will be considered in this precursor project. Colors correspond to missions' orbit repeat periods

3.1.14 Multispectral images

Concerning multispectral images, in general all the sites can be observed. The images close to the in-situ stations or under the virtual stations will be selected in the way to guarantee a complete coverage of the selected sites in case of clouds. For the analysis, multiple platforms will be considered to access and process the images. Landsat 7/8/9 images, and data from MODIS sensors onboard Aqua and Terra satellites will be processed using Google Earth Engine. Data from Sentinel-2/3 imagers will be accessed through Sentinel-Hub. For OLCI and MERIS, SNAP platform is going to be investigated for a fast process. About the sites already analysed in previous ESA projects (RIDESAT, STREAMRIDE, 4DMED-Hydrology), we have already analysed with Sentinel-2 and MODIS the following rivers: Amazon, Congo, Danube, Gange-Brahmaputra, Mississippi, Po. An attempt to merge the images from MERIS, Landsat 7 and MODIS has been already carried out along the Niger (Tarpanelli et al., 2019), whereas the combination of MODIS and OLCI along the Po River (Tarpanelli et al., 2020). For the rest of the rivers, new analyses will be done during the project (see Fig. 21).

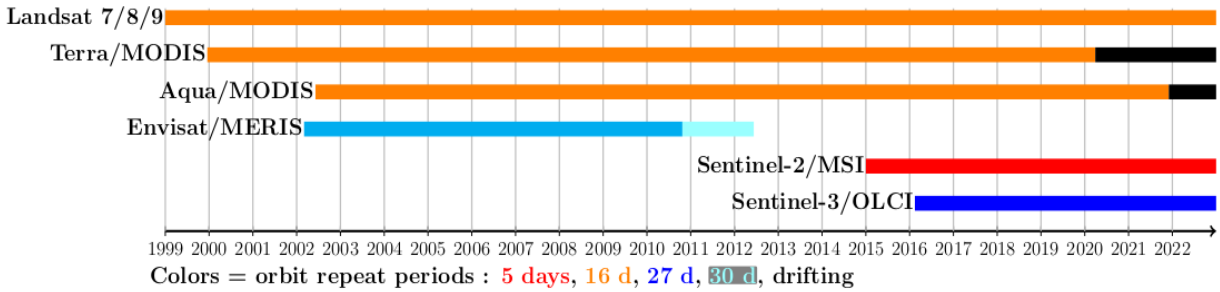

Figure 21. Timeline of the multispectral imagers that will be considered in this precursor project. Colors correspond to missions' orbit repeat periods

3.2 Expected data availability for each station

3.2.1 Amazon

The Figure 22 shows the available data over the entire basin and a timeline of the period of data availability for each selected stations of interest. Characteristics of each station are described in Table 2.

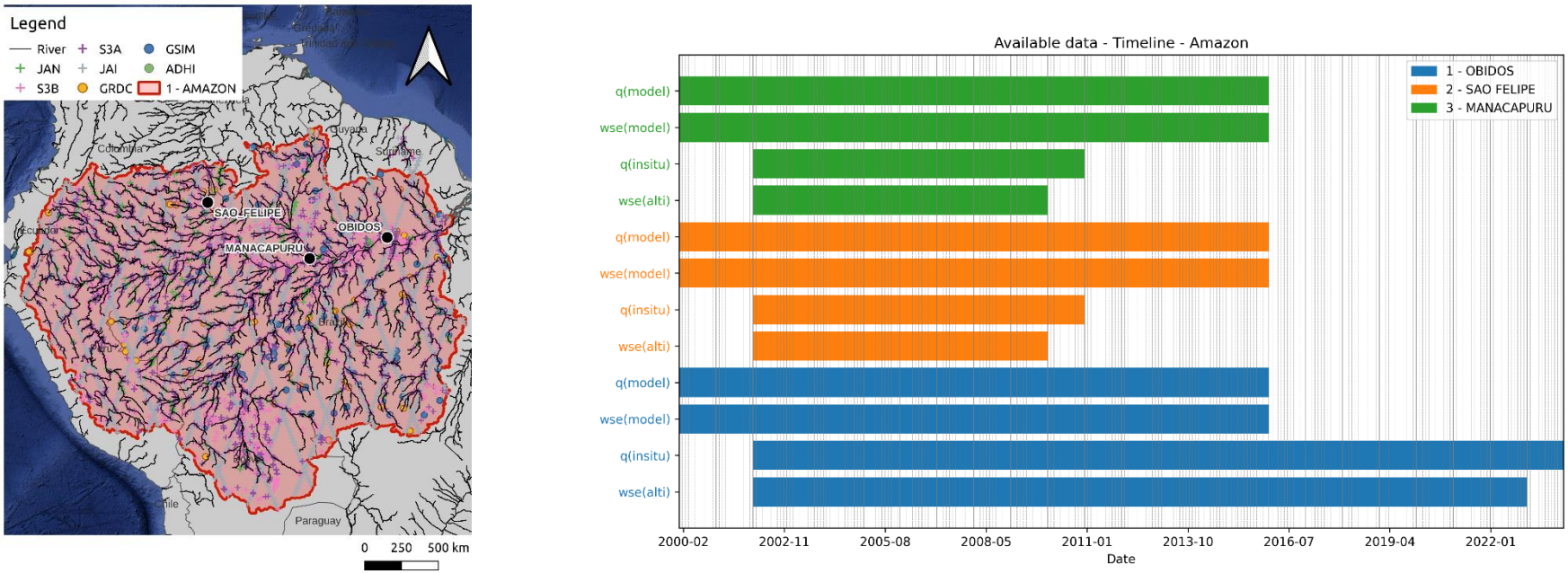

Figure 22. On the left side, the basin (red area) with main drainage network (black line), the available altimetry OLTC data from different constellations (cross) and in-situ gauges stations from different catalogues (colors points). On the right side, timeline of available data (WSE and discharge) for each selected stations of interest.

n°	Station name	River	Country	Lon	Lat	Drainage area (km²)	Period	Timestep	Source
1	OBIDOS	AMAZONA	BR	-55.51	-1.91	4670000	1968-2022	DAILY	ANA
2	SAO FELIPE	NEGRO	BR	-67.31	0.371	110862	1977-2022	DAILY	ANA
3	MANACAPURU	SOLIMOES	BR	-60.60	-3.31	2147736	1972-2022	DAILY	ANA

Table 2. Characteristics of each selected stations with position, river, drainage area, timestep, and period and sources of in-situ gauges.

In the Amazon River basin, the very complete in situ database, and the already processed time series of altimetry, ensures a quite complete overlap between each mission and in situ data, and also a good possibility of validating long-term discharge product.

3.2.2 Chad

The Figure 23 shows the available data over the entire basin and a timeline of the period of data availability for each selected stations of interest. Characteristics of each station are described in Table 3.

In the Chad River basin, the overlap with altimetry is mostly on ENVISAT or older missions. However, we hope more recent data can be accessed during the project in order to better validate our product. Modeled water level and flow data are also available for this basin over the period 1981-2022 from the MGB hydrological model [1].

[1] The MGB is a physically-based large-scale distributed hydrological model developed by the IPH (Collischonn et al. 2007a, Getirana et al. 2009, Paiva et al. 2011) of Porto Alegre (Brazil) and initially designed for large basins Brazilians and to overcome the limited in situ data available (Getirana et al. 2009). The model mainly produces time series of daily flows distributed at different points in space. To predict the distributed flow in a basin, time series of hydrometeorological variables, watershed elevation data, land cover and soil maps to represent physical and hydrological processes are needed (Paiva et al. 2011) .

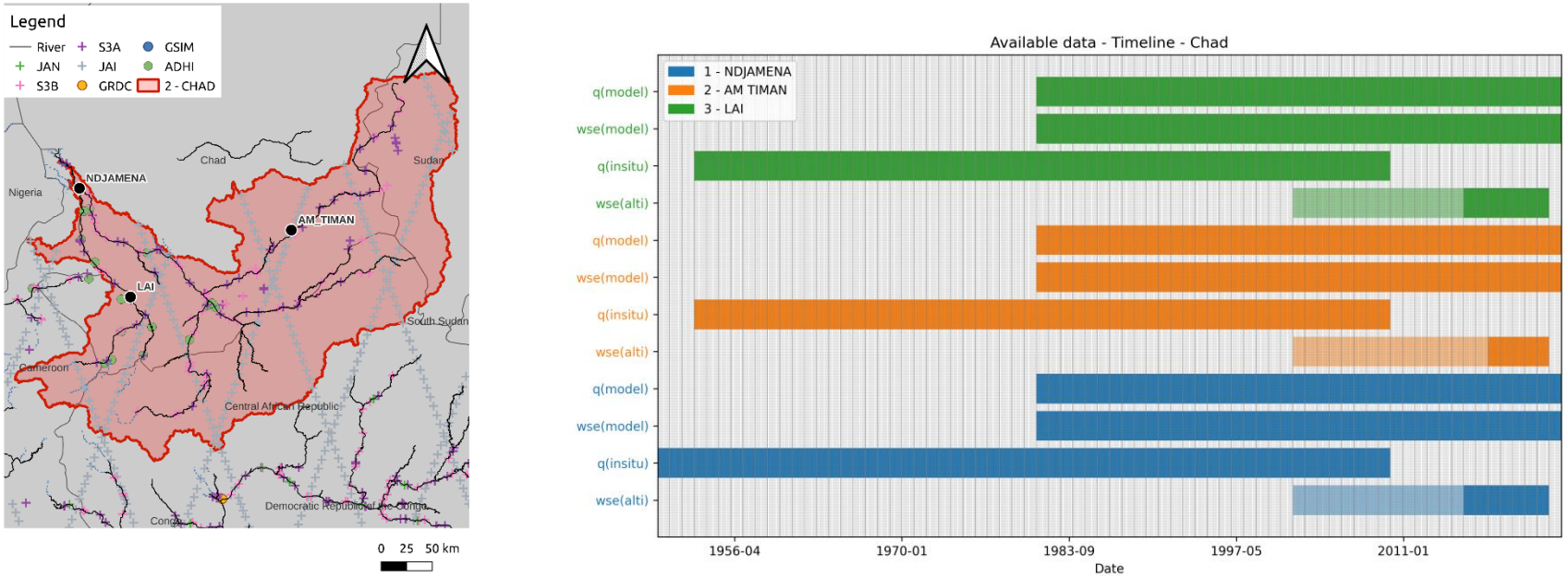

Figure 23. On the left side, the basin (red area) with main drainage network (black line), the available altimetry OLTC data from different constellations (cross) and in-situ gauges stations from different catalogues (colors points). On the right side, timeline of available data (WSE and discharge) for each selected stations of interest.

n°	Station name	River	Country	Lon	Lat	Drainage area (km²)	Period	Timestep	Source
1	NDJAMENA	CHARI	CH	15.03	12.10	600000	1950-2009	monthly	SIEREM
2	AM TIMAN	BAHR AZOUM	CH	20.3	11.06	NA	1953-2009	monthly	SIEREM
3	LAI	LOGONE	CH	16.3	9.4	56700	1953-2009	monthly	SIEREM

Table 3. Characteristics of each selected stations with position, river, drainage area, timestep, and period and sources of in-situ gauges.

3.2.3 Colville

The Figure 24 shows the available data over the entire basin and a timeline of the period of data availability for each selected stations of interest. Characteristics of each station are described in Table 4.

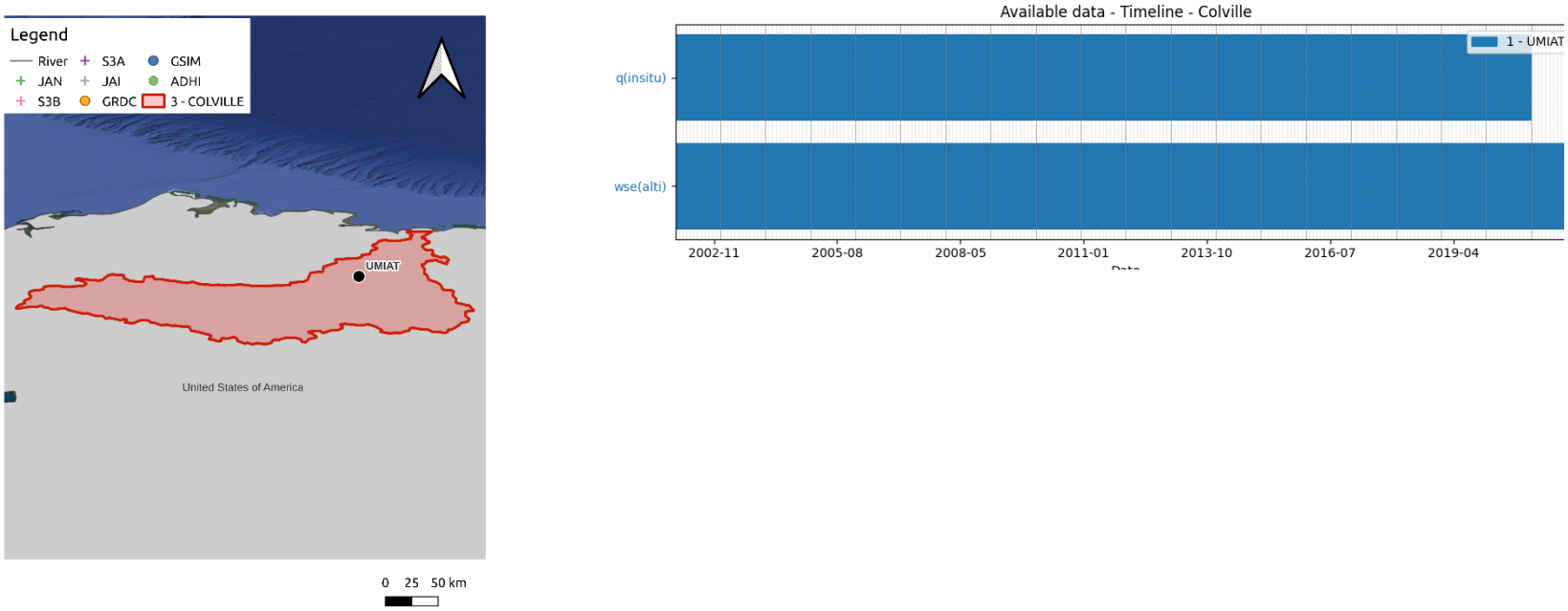

Figure 24. On the left side, the basin (red area) with main drainage network (black line), the available altimetry OLTC data from different constellations (cross) and in-situ gauges stations from different catalogues (colors points). On the right side, timeline of available data (WSE and discharge) for each selected stations of interest.

n°	Station name	River	Country	Lon	Lat	Drainage area (km²)	Period	Timestep	Source
1	UMIAT	COLVILLE	US	-152.12	69.36	35820	2002-2020	daily	USGS

Table 4. Characteristics of each selected stations with position, river, drainage area, timestep, and period and sources of in-situ gauges.

The Colville River is typical middle size Arctic river with large (1.5-2 km) braided channel. No altimetric WSE time series have been retrieved for this river. Nevertheless, for several rivers of similar fluvial geomorphology (Yukon, Pur and Nadym rivers) adequate WSE time series from ENVISAT and Sentinel-3 measurements were already built.

3.2.4 Congo

The Figure 25 shows the available data over the entire basin and a timeline of the period of data availability for each selected stations of interest. Characteristics of each station are described in Table 5.

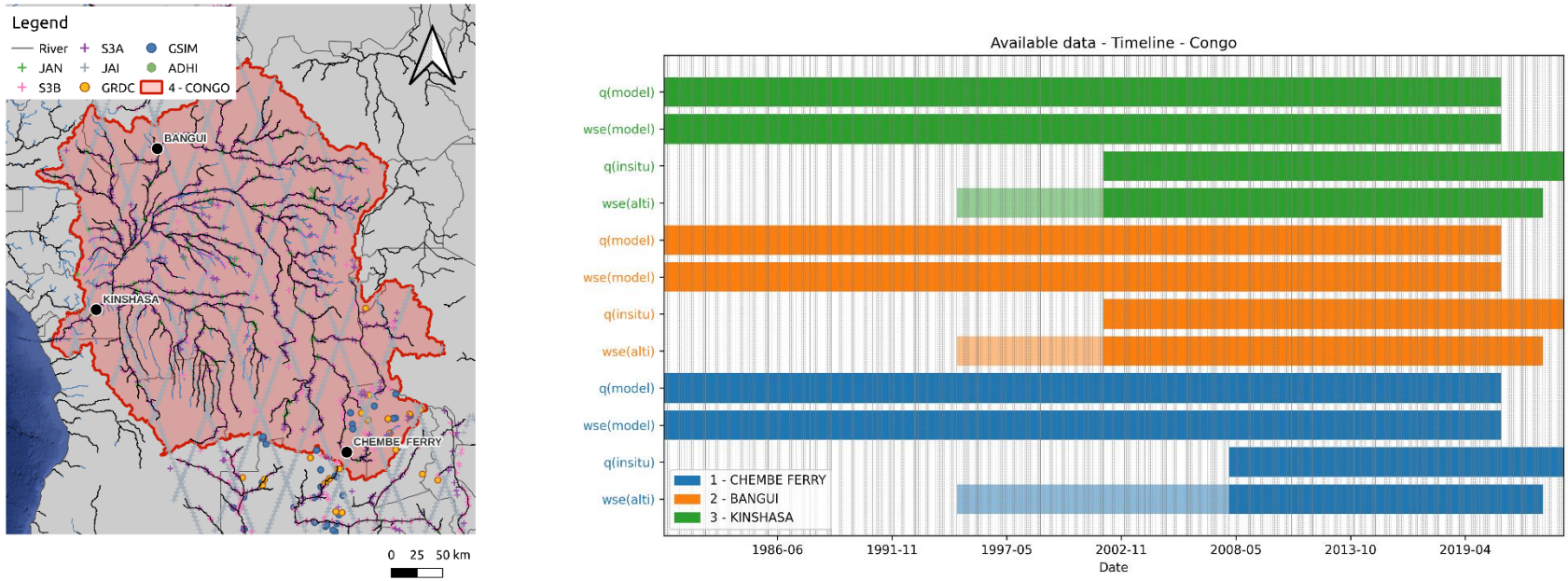

Figure 25. On the left side, the basin (red area) with main drainage network (black line), the available altimetry OLTC data from different constellations (cross) and in-situ gauges stations from different catalogues (colors points). On the right side, timeline of available data (WSE and discharge) for each selected stations of interest.

n°	Station name	River	Country	Lon	Lat	Drainage area (km²)	Period	Timestep	Source
1	CHEMBE FERRY	LUAPULA	ZM	28.75	-11.9	123072	1956-2005	daily	GRDB
2	BANGUI	UBANGI	CF	18.58	4.36	499000	1911-2016	daily	GRDB
3	KINSHASA	CONGO	CD	15.3	-4.3	3475000	1903-2010	daily	GRDB

Table 5. Characteristics of each selected stations with position, river, drainage area, timestep, and period and sources of in-situ gauges.

Data availability in the CRB is an issue not only regarding water levels and discharge estimates, but also for other variables such as precipitation. Most of in situ-based datasets provide either mean monthly values or historical series (Alsdorf et al., 2016). Satellite estimates, especially those based on the GPM constellation, have proved to be a credible alternative to compensate the lack of in-situ data.

Lots of satellite altimetry data are available on this basin: Jason-2 and 3, ENVISAT, SARAL, and Sentinel-3 missions. The spans for the WSE time series are 2002–2010 for ENVISAT, 2008–2016 for Jason-2, 2013–2016 for SARAL, and 2016–present for Jason-3 and Sentinel-3A missions.

In addition, modeled water level and flow data are also available for this basin over the period 1981-2020 from the MGB hydrological model.

3.2.5 Danube

The Figure 26 shows the available data over the entire basin and a timeline of the period of data availability for each selected stations of interest. Characteristics of each station are described in Table 6.

In situ Water levels and discharge on the Danube are freely available online from the Bayerisches Landesamt für Umwelt website. At Baja station, there is a strong overlap with satellite data, and at this location the International Commission for the Protection of the *Danube* River (*ICPDR*) also provides in situ data. On the others the overlap is smaller, yet still interesting, with few years of Jason-2 and full ENVISAT period.

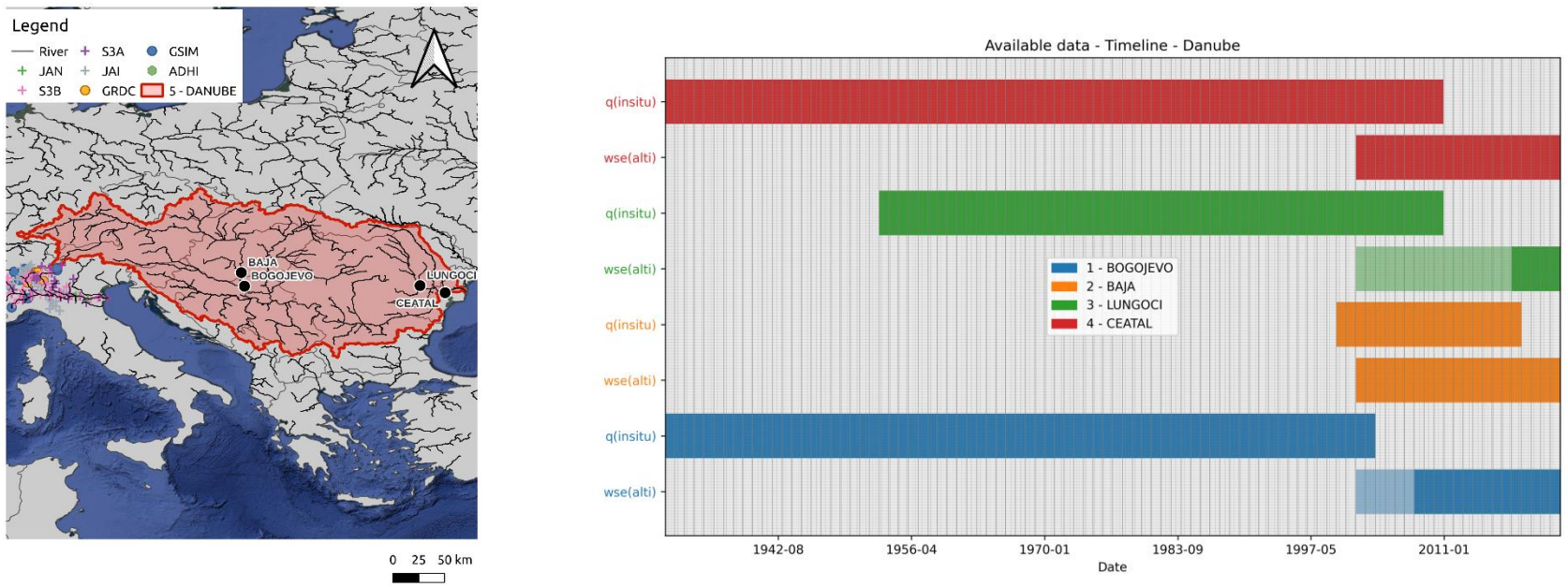

Figure 26. On the left side, the basin (red area) with main drainage network (black line), the available altimetry OLTC data from different constellations (cross) and in-situ gauges stations from different catalogues (colors points). On the right side, timeline of available data (WSE and discharge) for each selected stations of interest.

n°	Station name	River	Country	Lon	Lat	Drainage area (km²)	Period	Timestep	Source
1	BOGOJEVO	DANUBE	SR	19.08	45.53	251593	1931-2003	daily	GRDB
2	BAJA	DANUBE	HU	18.93	46.18	208282	2000 - 2018	daily	ICPDR
3	LUNGOCI	SIRET	RO	27.51	45.55	36000	1953-2010	daily	GRDB
4	CEATAL	DANUBE	RO	28.71	45.21	807000	1931-2010	daily	GRDB

Table 6. Characteristics of each selected stations with position, river, drainage area, timestep, and period and sources of in-situ gauges.

3.2.6 Ganga-Brahmaputra

The Figure 27 shows the available data over the entire basin and a timeline of the period of data availability for each selected stations of interest. Characteristics of each station are described in Table 7.

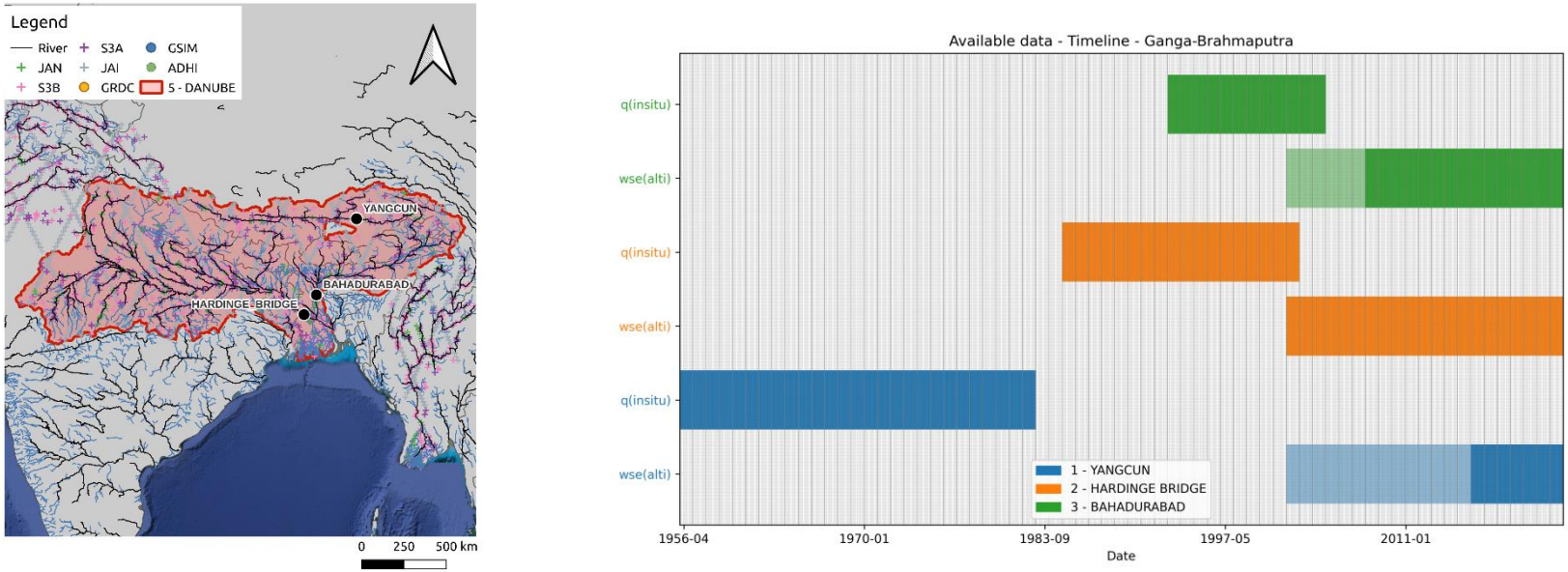

Figure 27. On the left side, the basin (red area) with main drainage network (black line), the available altimetry OLTC data from different constellations (cross) and in-situ gauges stations from different catalogues (colors points). On the right side, timeline of available data (WSE and discharge) for each selected stations of interest.

n°	Station name	River	Country	Lon	Lat	Drainage area (km²)	Period	Timestep	Source
1	YANGCUN	BRAHMAPUTRA	CH	91.88	29.28	153191	1956-1982	daily	GRDB
2	HARDINGE BRIDGE	GANGE	BD	89.03	24.08	9450000	1985-2002	daily	GRDB/ BWDB
3	BAHADURABAD	BRAHMAPUTRA	BD	89.7	25.15	520000	1993-2004	daily	BWDB

Table 7. Characteristics of each selected stations with position, river, drainage area, timestep, and period and sources of in-situ gauges. OBJ

Discharge in-situ data are available at three stations: Yangcun with daily discharge from 1956 to 1982, Hardinge Bridge with daily discharge from 1985 to mid-2002 and at Bahadurabad with daily discharge from 1993 to 2004. As well as WSE in-situ data with 858 infrequent measurements for the Ganga from May 2006 to August 2011 and 102 infrequent measurements for the Brahmaputra from January 2008 to August 2011 (See Papa et al., 2012). Over these three stations, multispectral datasets are also available.

3.2.7 Garonne

The Figure 28 shows the available data over the entire basin and a timeline of the period of data availability for each selected stations of interest. Characteristics of each station are described in Table 8.

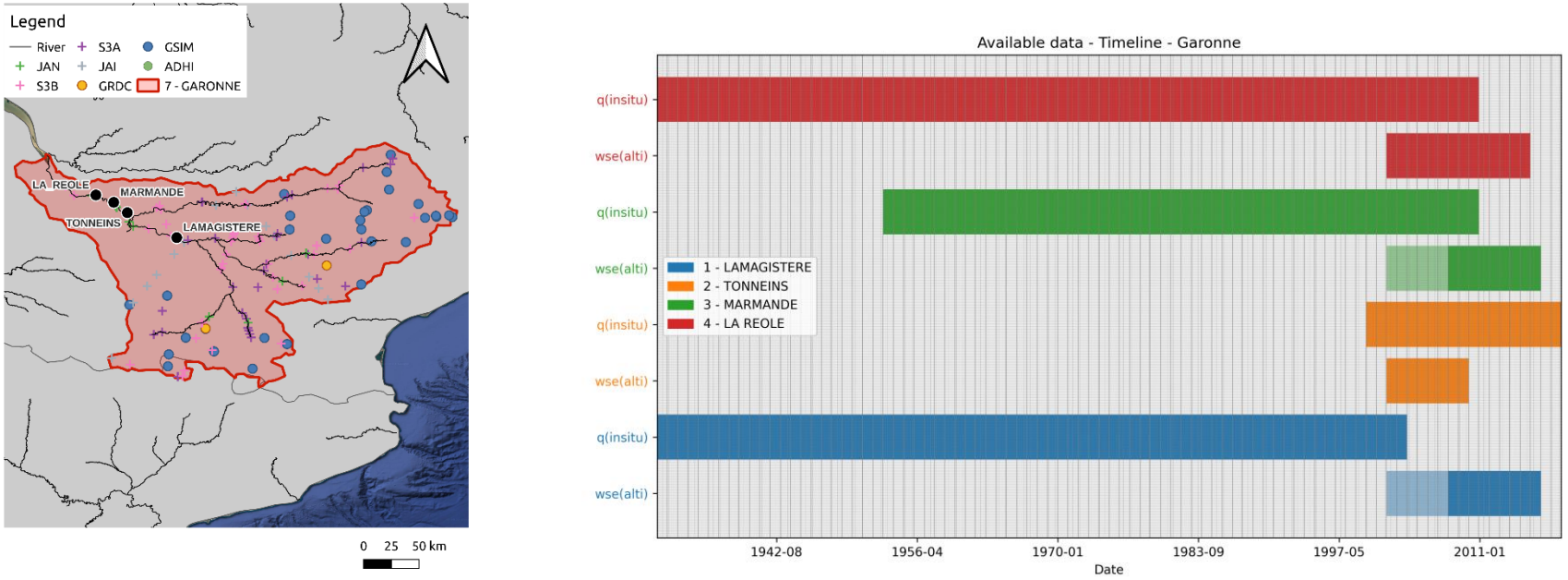

Figure 28. On the left side, the basin (red area) with main drainage network (black line), the available altimetry OLTC data from different constellations (cross) and in-situ gauges stations from different catalogues (colors points). On the right side, timeline of available data (WSE and discharge) for each selected stations of interest.

n°	Station name	River	Country	Lon	Lat	Drainage area (km²)	Period	Timestep	Source
1	LAMAGISTERE	GARONNE	FR	0.83	44.12	32350	1966-2023	daily	SCHAPI
2	TONNEINS	GARONNE	FR	0.30	44.38	50100	1989-2023	daily	SCHAPI
3	MARMANDE	GARONNE	FR	0.15	44.49	50670	1986-2023	daily	SCHAPI
4	LA REOLE	GARONNE	FR	-0.03	44.57	51480	2013-2023	daily	SCHAPI

Table 8. Characteristics of each selected stations with position, river, drainage area, timestep, and period and sources of in-situ gauges.

Discharge in-situ data, as well as WSE, are available at four stations: Lamagistere, Tonneins, Marmande and La reole with daily discharge time series from earlier than 1990 to now. Some additional data could be requested to DREAL.

Jason-3/2 and Envisat time series have already been computed on the basin (magenta and red dots on Fig. 8, see Biancamaria et al., 2017). The availability of multispectral datasets should be available, but clouds might be an issue!

3.2.8 Indus

The Figure 29 shows the available data over the entire basin and a timeline of the period of data availability for each selected stations of interest. Characteristics of each station are described in Table 9.

In situ daily data are available during the monsoon period, at different locations along the Indus River networks, within the Annual Flood Reports, from the Federal Flood Commission (FFC) from the Ministry of Water Resources from the Government of Pakistan. In particular, daily discharge upstream and downstream the reservoirs at Tarbela (drainage area ~200 000 km²), Guddu (drainage area ~900 000 km²), and Kotri (drainage area ~1.1 million km²) (see Fig. 29) are available for monsoon periods from 2012 to 2018.

Some altimetry times series from Jason-2, Jason-3 and Sentinel-3A/B have been computed near Tarbela and Guddu. Envisat data have not yet been processed, but according to the available ground tracks (see dotted red line on Fig. 29), it should be possible to get some interesting data near these dams.

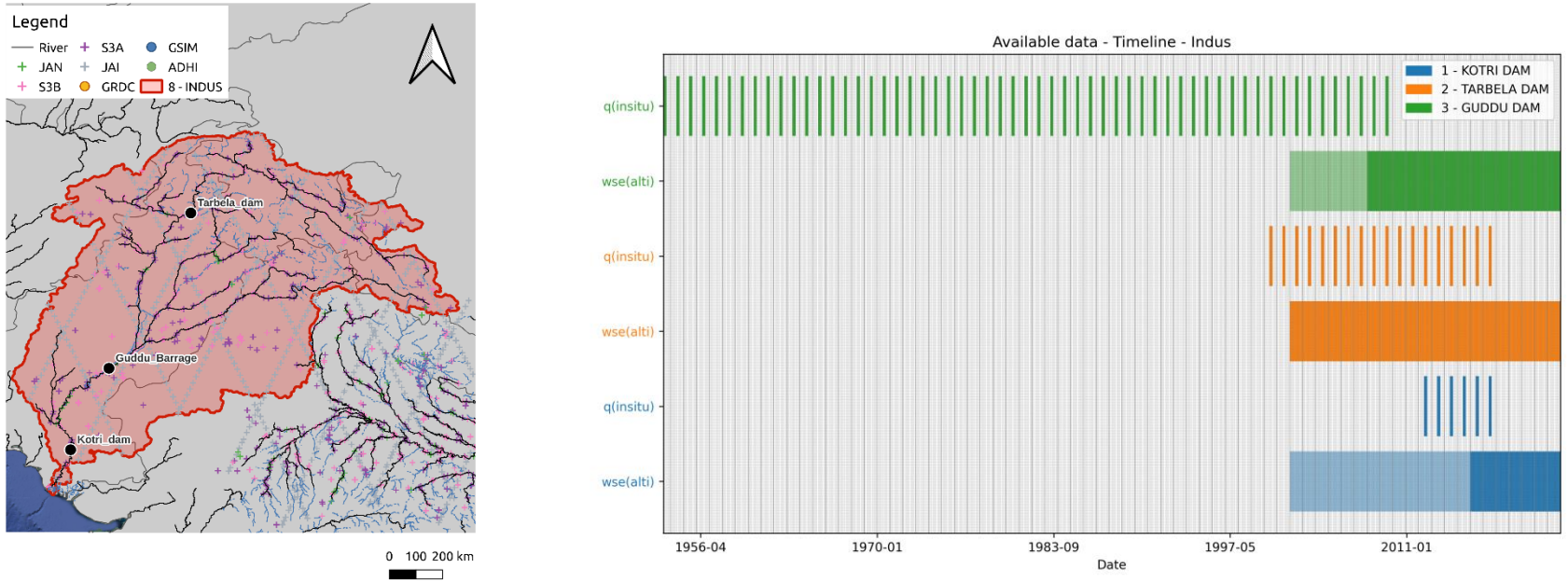

Figure 29. On the left side, the basin (red area) with main drainage network (black line), the available altimetry OLTC data from different constellations (cross) and in-situ gauges stations from different catalogues (colors points). On the right side, timeline of available data (WSE and discharge) for each selected stations of interest.

n°	Station name	River	Country	Lon	Lat	Drainage area (km²)	Period	Timestep	Source
1	KOTRI DAM	INDUS	PK	68.31	25.44	1100000	2012-2018 (monsoon)	daily	FFC
2	TARBELA DAM	INDUS	PK	72.69	34.08	200000	2012-2018 (monsoon)	daily	FFC
3	GUDDU DAM	INDUS	PK	69.71	28.41	900000	2012-2018 (monsoon)	daily	FFC

Table 9. Characteristics of each selected stations with position, river, drainage area, timestep, and period and sources of in-situ gauges.

3.2.9 Irrawaddy

The Figure 30 shows the available data over the entire basin and a timeline of the period of data availability for each selected stations of interest. Characteristics of each station are described in Table 10.

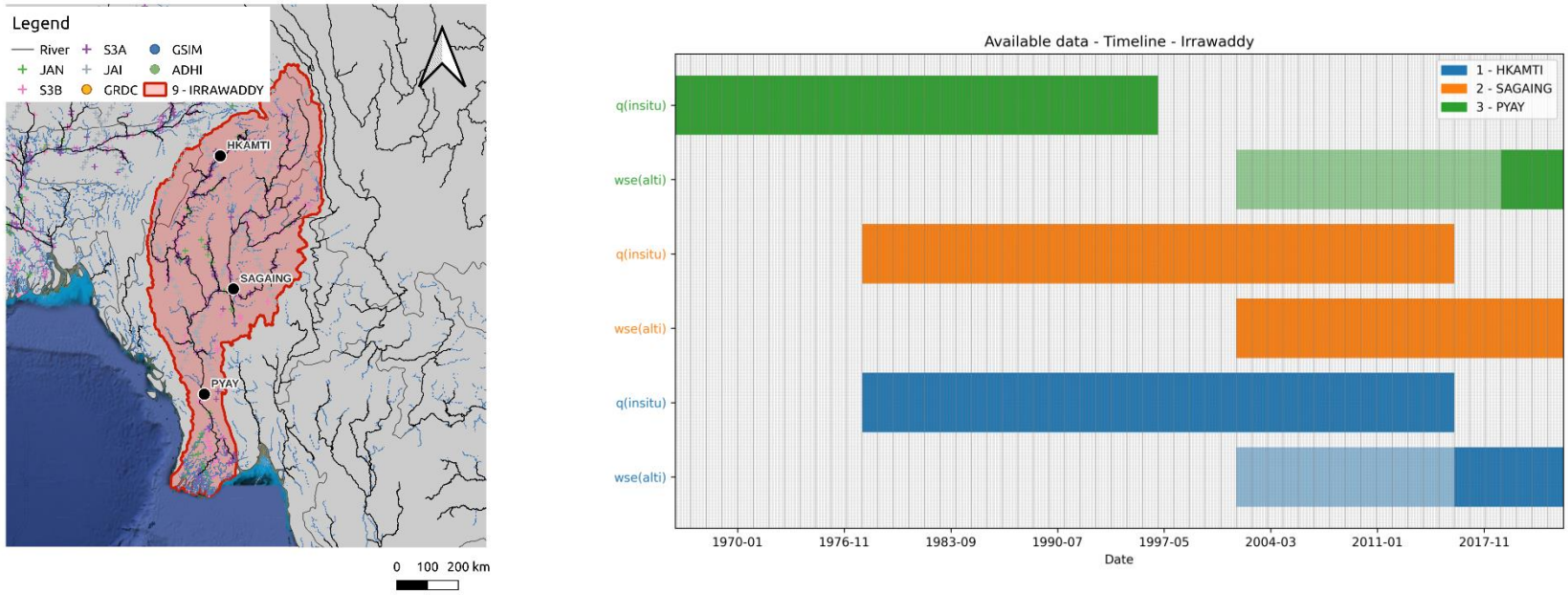

Figure 30. On the left side, the basin (red area) with main drainage network (black line), the available altimetry OLTC data from different constellations (cross) and in-situ gauges stations from different catalogues (colors points). On the right side, timeline of available data (WSE and discharge) for each selected stations of interest.

n°	Station name	River	Country	Lon	Lat	Drainage area (km²)	Period	Timestep	Source
1	HKAMTI	CHINDWIN	MM	95.7	26	27420	1978-2015	daily	GRDB
2	SAGAING	IRRAWADDY	MM	96.09	21.98	120193	1978-2015	daily	GRDB
3	PYAY	IRRAWADDY	MM	95.26	18.84	340,390	1966-1996	monthly	Furuichi et al. (2009)

Table 10. Characteristics of each selected stations with position, river, drainage area, timestep, and period and sources of in-situ gauges.

At the most downstream station (namely PYAY), we only have few years of recovering with T/P data (1993-1996). On the other two stations we choose, there is data available until 2015 which is quite favourable to compare with Jason-2 data.

3.2.10 Lena

The Figure 31 shows the available data over the entire basin and a timeline of the period of data availability for each selected stations of interest. Characteristics of each station are described in Table 11.

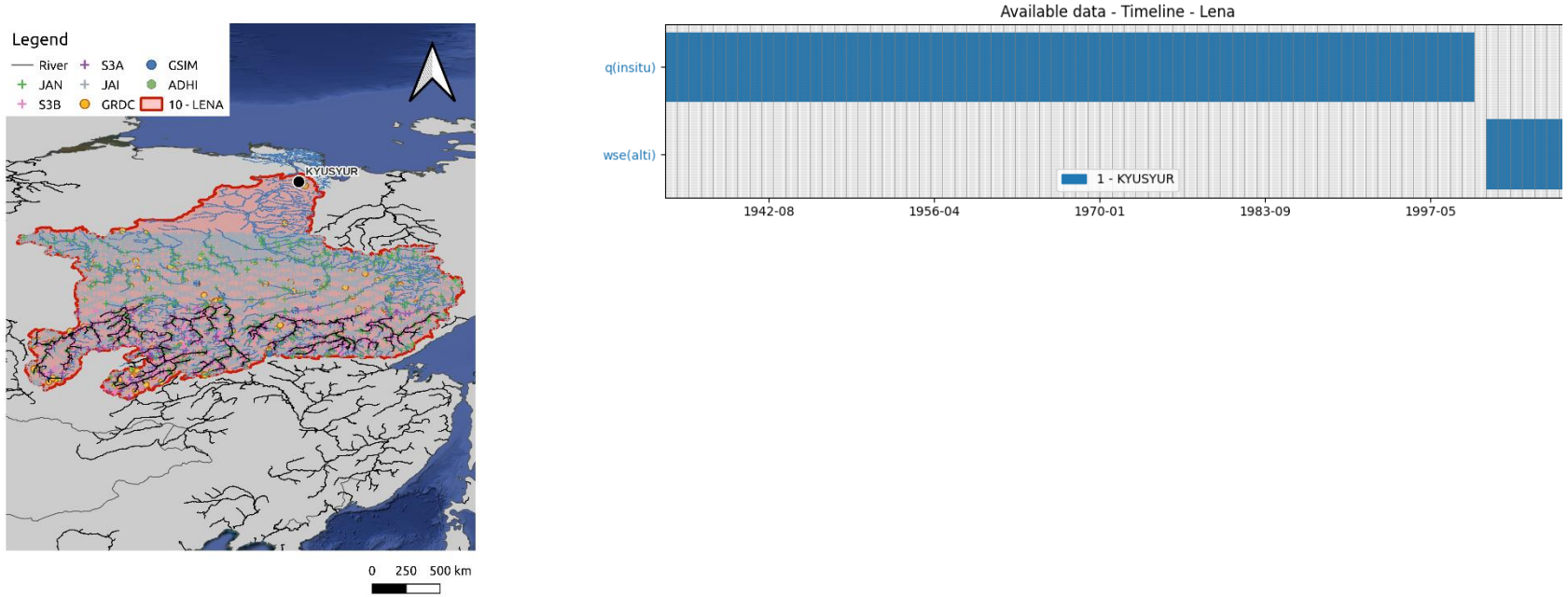

Figure 31. On the left side, the basin (red area) with main drainage network (black line), the available altimetry OLTC data from different constellations (cross) and in-situ gauges stations from different catalogues (colors points). On the right side, timeline of available data (WSE and discharge) for each selected stations of interest.

n°	Station name	River	Country	Lon	Lat	Drainage area (km²)	Period	Timestep	Source
1	KYUSYUR	LENA	RU	127.39	70.68	2430000	1934-2000	daily	GRDB

Table 11. Characteristics of each selected stations with position, river, drainage area, timestep, and period and sources of in-situ gauges.

Lena River in lower reaches is covered only by polar orbiting missions (ENVISAT, AltiKa and Sentinel-3). Due to high banks and narrow valley the WSE time series of ENVISAT have many gaps. The Sentinel-3 WSE after 2019 are complete and have demonstrated the accuracy acceptable for discharge retrievals. To overcome the scarcity of the altimetric data at river outlet, the Jason-2, and-3 WSE measurements (located in 700 km from the delta in area with large valley and low banks) could be used for the discharge estimations.

3.2.11 Limpopo

The Figure 32 shows the available data over the entire basin and a timeline of the period of data availability for each selected stations of interest. Characteristics of each station are described in Table 12.

In the Limpopo River basin, the most downstream station does not have any observation since 1988. However, this is quite critical, we choose to keep this station since it is the one that will provide information of ocean inflow, as pointed-out by the URD. We will try to obtain more data at this location. If nothing can be obtained, we can state that the discharge product from space will serve strongly to ensure an almost continuous time series from past to present, bridging the gap between past in situ data and current observation.

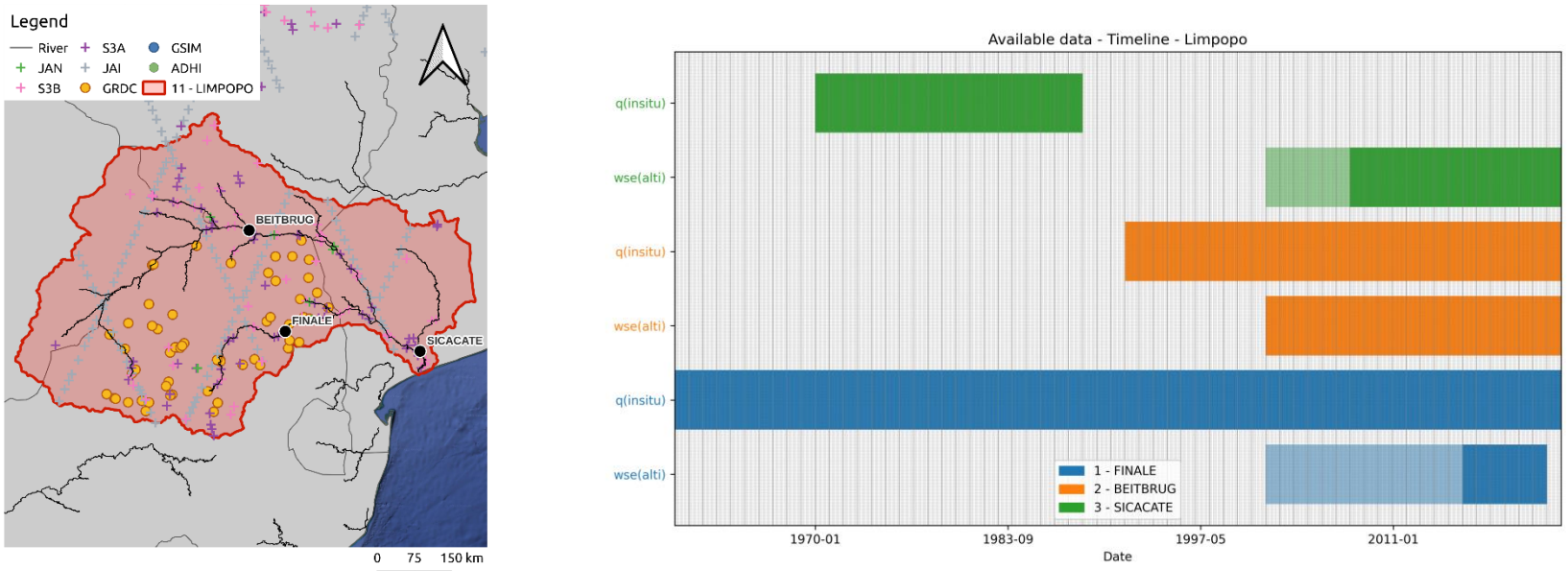

Figure 32. On the left side, the basin (red area) with main drainage network (black line), the available altimetry OLTC data from different constellations (cross) and in-situ gauges stations from different catalogues (colors points). On the right side, timeline of available data (WSE and discharge) for each selected stations of interest.

n°	Station name	River	Country	Lon	Lat	Drainage area (km²)	Period	Timestep	Source
1	FINALE	OLIFANTSRIVIER	ZA	30.74	-24.33	42714	1960-2022	daily	GRDB
2	BEITBRUG	LIMPOPO	ZA	29.99	-22.22	201001	1992-2022	daily	GRDB
3	SICACATE	LIMPOPO	ZM	33.54	-24.74	416522	1970-1988	daily	GRDB

Table 12. Characteristics of each selected stations with position, river, drainage area, timestep, and period and sources of in-situ gauges.

3.2.12 Mackenzie

The Figure 33 shows the available data over the entire basin and a timeline of the period of data availability for each selected stations of interest. Characteristics of each station are described in Table 13.

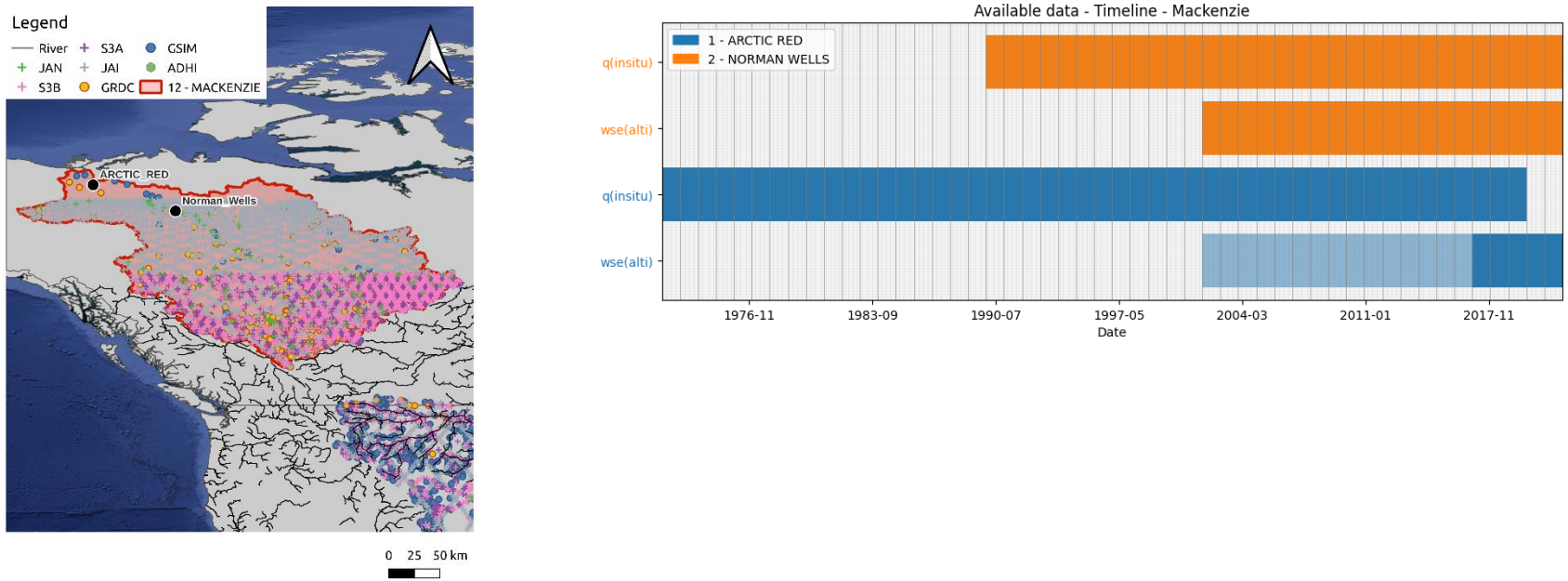

Figure 33. On the left side, the basin (red area) with main drainage network (black line), the available altimetry OLTC data from different constellations (cross) and in-situ gauges stations from different catalogues (colors points). On the right side, timeline of available data (WSE and discharge) for each selected stations of interest.

n°	Station name	River	Country	Lon	Lat	Drainage area (km²)	Period	Timestep	Source
1	ARCTIC RED	MACKENZIE	CA	-133.74	67.45	1660000	1972-2019	daily	GRDB
2	NORMAN WELLS	MACKENZIE	CA	-126.85	65.27		1990-2021	daily	HyDat

Table 13. Characteristics of each selected stations with position, river, drainage area, timestep, and period and sources of in-situ gauges.

In-situ discharge is available for 1990-2020. Between 1996 and 2000 the winter discharges were not measured. Sentinel-3 onboard DEM was wrong before 2020 in area northward from 66°N (upper stream from the gauging station). So, only 1-2 adequate WSE measurements per year can be extracted. Several S3 virtual stations could be good at 62°N. The area between 62°N and 66°N takes an exploration. The river reach near Normann Well gauging station is covered by 10-days Jason observations. Successful ENVISAT WSE time series exist for the Mackenzie delta. They can be used for discharge retrievals.

3.2.13 Maroni

The Figure 34 shows the available data over the entire basin and a timeline of the period of data availability for each selected stations of interest. Characteristics of each station are described in Table 14.

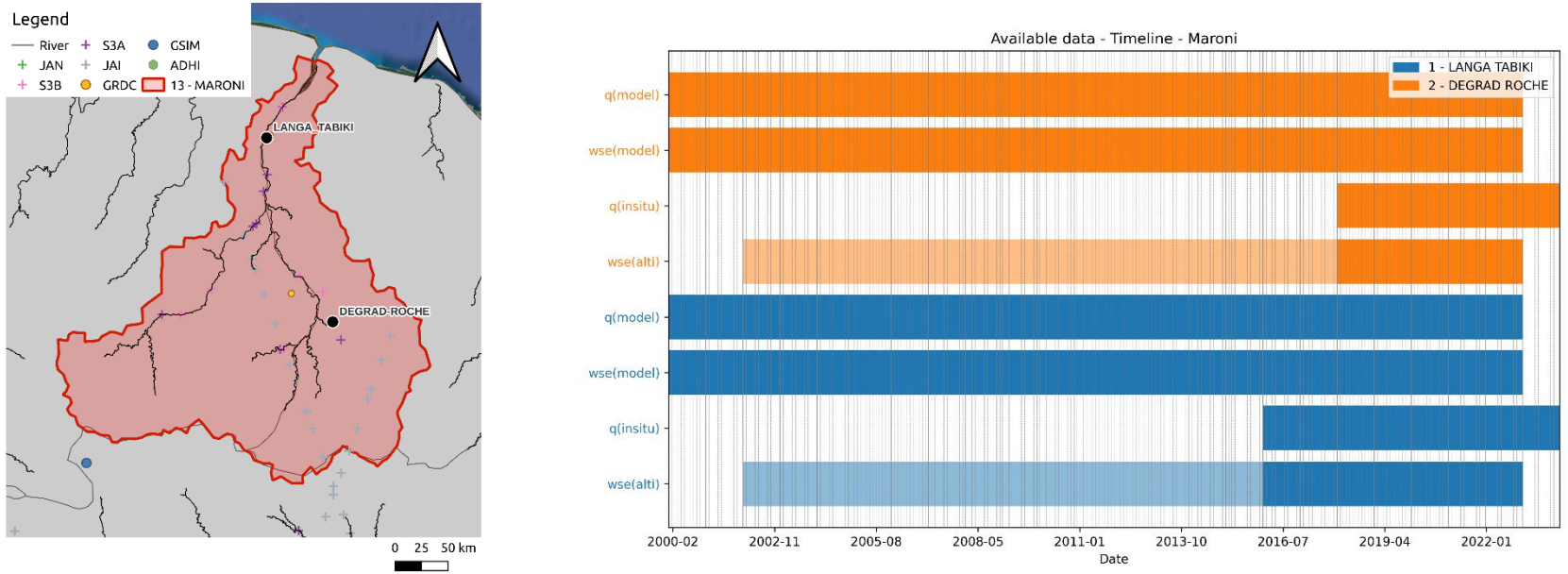

Figure 34. On the left side, the basin (red area) with main drainage network (black line), the available altimetry OLTC data from different constellations (cross) and in-situ gauges stations from different catalogues (colors points). On the right side, timeline of available data (WSE and discharge) for each selected stations of interest.

n°	Station name	River	Country	Lon	Lat	Drainage area (km²)	Period	Timestep	Source
1	LANGA TABIKI	MARONI	GF	-54.43	4.98	60930	1950-2022	daily	SCHAPI
2	DEGRAD-ROCHE	TAMPOK	GF	-53.86	3.42	7650	1950-2022	daily	SCHAPI

Table 14. Characteristics of each selected stations with position, river, drainage area, timestep, and period and sources of in-situ gauges.

The long-term data available in the Maroni River basin are obtained from SCHAPI. Both sites are followed with good maintenance actions and SCHAPI provides the list of changes that could have affected the quality of the data, together with a quality status. This should ensure that the long-term time series are consistent and can be used straightforward for the needs of the project.

In addition, modeled water level and flow data are also available for this basin over the period 2000-2022 from the MGB hydrological model.

3.2.14 Mississippi

The Figure 35 shows the available data over the entire basin and a timeline of the period of data availability for each selected stations of interest. Characteristics of each station are described in Table 15.

In situ water level and/or discharge over the Mississippi basin are freely available for hundreds of gages on the USGS website. Especially, Gehring et al. 2022 estimated that nearly 500 active sites with at least daily data are available from the USGS National Water Information System (NWIS) for the period 2001–2021. They also associated 230 of these gages to a nearby S3A/B time series available on Hydroweb. Historical missions have already been used at some location to derive the river WSE (e.g., Coss et al., 2020), so there is no doubt that current S3A/B tile series from Hydroweb can be extended using other altimetry missions.

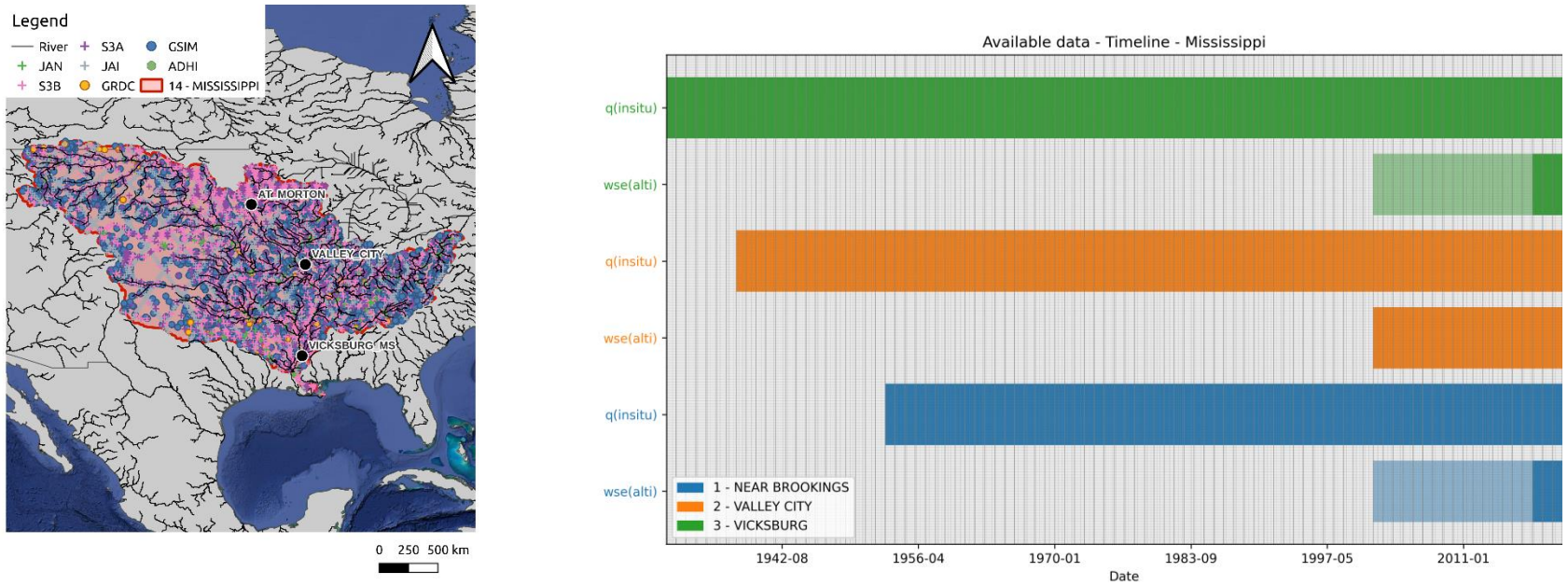

Figure 35. On the left side, the basin (red area) with main drainage network (black line), the available altimetry OLTC data from different constellations (cross) and in-situ gauges stations from different catalogues (colors points). On the right side, timeline of available data (WSE and discharge) for each selected stations of interest.

n°	Station name	River	Country	Lon	Lat	Drainage area (km²)	Period	Timestep	Source
1	NEAR BROOKINGS	BIG SIOUX	US	-96.74	44.18	10095	1953-2021	daily	USGS
2	VALLEY CITY	ILLINOIS	US	-90.64	39.70	69267	1938-2021	daily	USGS
3	VICKSBURG, MS	MISSISSIPI	US	-90.90	32.31	2964255	1931-2021	daily	GRDB

Table 15. Characteristics of each selected stations with position, river, drainage area, timestep, and period and sources of in-situ gauges.

3.2.15 Niger

The Figure 36 shows the available data over the entire basin and a timeline of the period of data availability for each selected stations of interest. Characteristics of each station are described in Table 16.

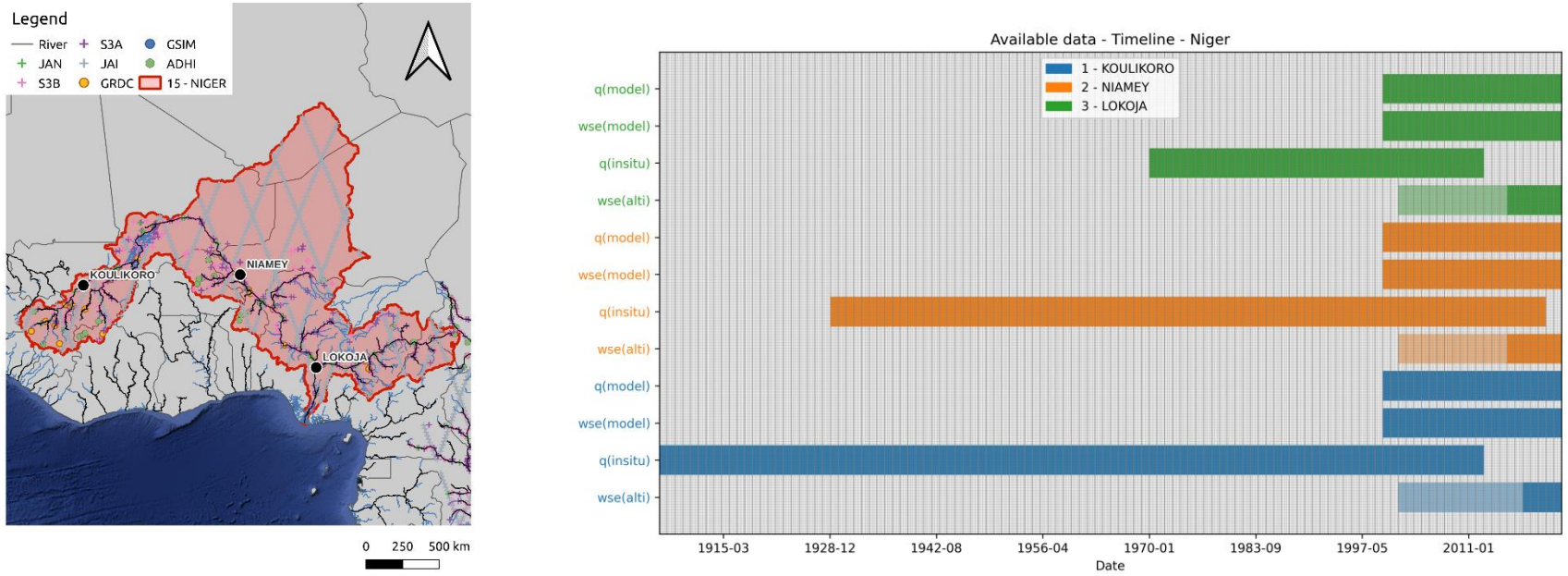

Figure 36. On the left side, the basin (red area) with main drainage network (black line), the available altimetry OLTC data from different constellations (cross) and in-situ gauges stations from different catalogues (colors points). On the right side, timeline of available data (WSE and discharge) for each selected stations of interest.

n°	Station name	River	Country	Lon	Lat	Drainage area (km²)	Period	Timestep	Source
1	KOULIKORO	NIGER	ML	-7.55	12.86	120000	1907-2012	daily	GRDB
2	NIAMEY	NIGER	NE	2.09	13.52	700000	1929-2020	daily	GRDB
3	LOKOJA	NIGER	NG	6.7667	7.8	-	1970-2012	daily	GRDB

Table 16. Characteristics of each selected stations with position, river, drainage area, timestep, and period and sources of in-situ gauges.

The three stations points have been selected along the Niger river: 1) one at the river upstream: Koulikoro station 2) one at Niamey city level: Niamey station and the last one 3) at the outlet (confluence between Niger river and Benoué river): Lokoja station

For these 3 points, discharge and WSE from hydrological modelling are also available thank to MGB model over the period 2000-2022 at a daily timestep (Collischonn et al. 2007a, Getirana et al. 2009, Paiva et al. 2011)

3.2.16 Ob

The Figure 37 shows the available data over the entire basin and a timeline of the period of data availability for each selected stations of interest. Characteristics of each station are described in Table 17.

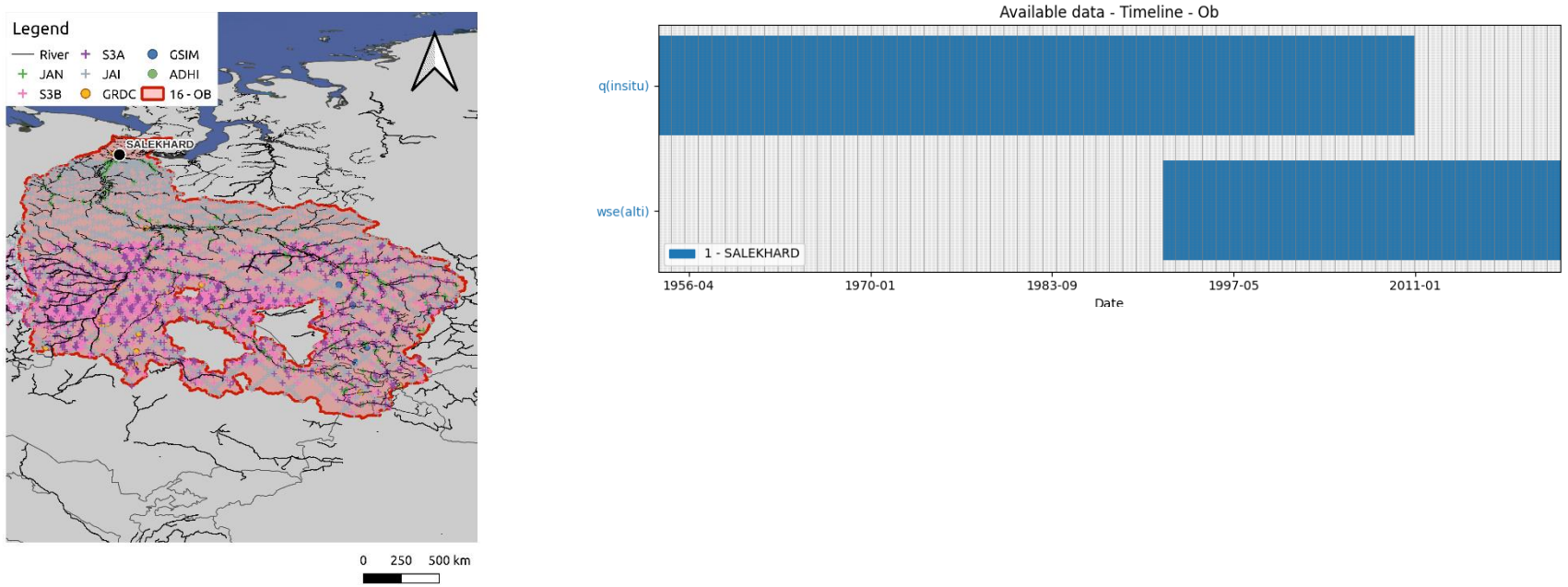

Figure 37. On the left side, the basin (red area) with main drainage network (black line), the available altimetry OLTC data from different constellations (cross) and in-situ gauges stations from different catalogues (colors points). On the right side, timeline of available data (WSE and discharge) for each selected stations of interest.

n°	Station name	River	Country	Lon	Lat	Drainage area (km²)	Period	Timestep	Source
1	SALEKHARD	OB	RU	66.59	66.62	2950000	1954-2010	daily	GRDB

Table 17. Characteristics of each selected stations with position, river, drainage area, timestep, and period and sources of in-situ gauges.

For the lower reaches of Ob River the WSE altimetric time series starts from the Topex/Poseidon period (end of 1992). Later missions of this series (Jason-2 and Jason-3) also have demonstrated a performance sufficient for discharge-related task. At least 4 complete WSE time series were built from the ENVISAT measurements and two of them were already used for the discharge retrievals. WSE retrieved from Sentinel-3A and –3B missions in this region also suitable for discharge calculations.

3.2.17 Po

The Figure 38 shows the available data over the entire basin and a timeline of the period of data availability for each selected stations of interest. Characteristics of each station are described in Table 18.

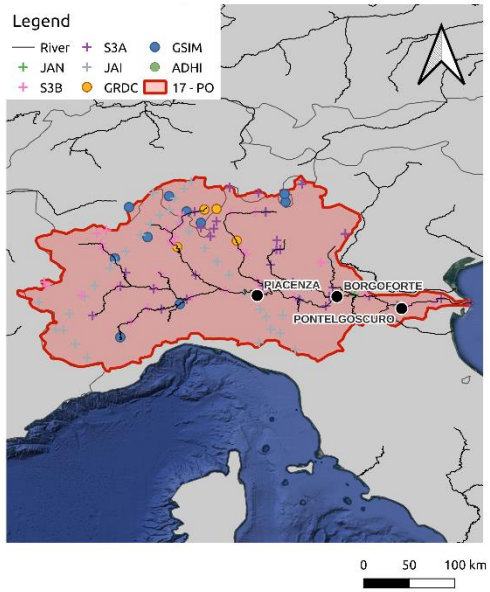

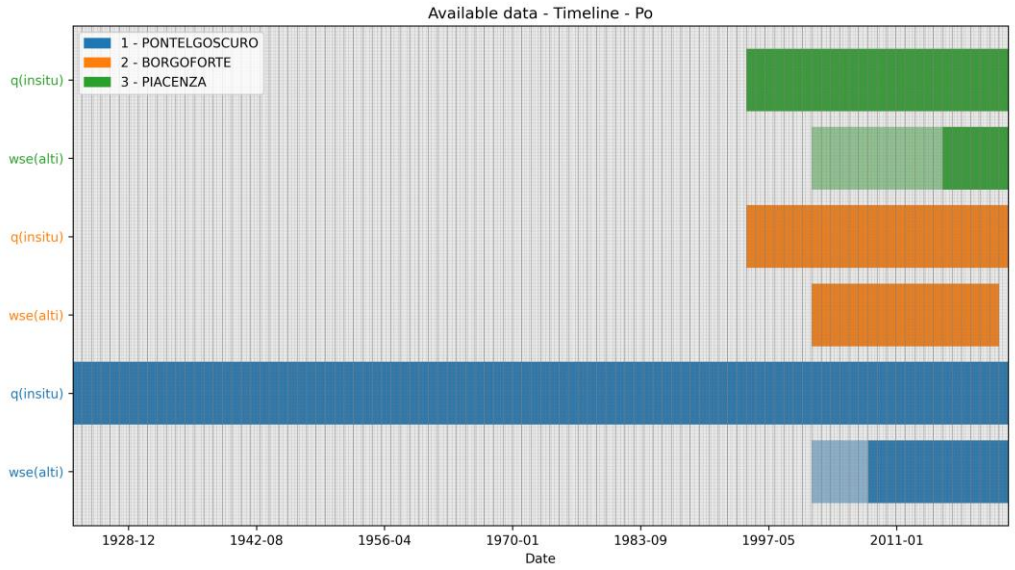

Figure 38. On the left side, the basin (red area) with main drainage network (black line), the available altimetry OLTC data from different constellations (cross) and in-situ gauges stations from different catalogues (colors points). On the right side, timeline of available data (WSE and discharge) for each selected stations of interest.

n°	Station name	River	Country	Lon	Lat	Drainage area (km²)	Period	Timestep	Source
1	PONTELGOSCURO	PO	IT	11.60	44.88	70091	1923-2022	daily	AIPo
2	BORGOFORTE	PO	IT	10.75	45.04	62450	1995-2022	daily	AIPo
3	PIACENZA	PO	IT	9.70	45.06	42030	1995-2022	daily	AIPo

Table 18. Characteristics of each selected stations with position, river, drainage area, timestep, and period and sources of in-situ gauges.

For the Po River, in situ data on river discharge and water level have been collected for several years. For the station of Pontelagoscuro, the last station before the influence of the Adriatic Sea on the river, IRPI has collected discharge data for about 100 years (from 1923). However, free data are available, for most of the stations from 1995 until the last year (2021). The process of validating the data and updating of the rating curve takes more than a year. However, unofficial data are also available for 2022.

3.2.18 Zambezi

The Figure 39 shows the available data over the entire basin and a timeline of the period of data availability for each selected stations of interest. Characteristics of each station are described in Table 19.

In the Zambezi River basin, the in-situ data is very scares, and nothing is publicly available on the databases. Also, the most recent data is from almost 20 years ago (2005 at Kabompo Pontoon). We will try to identify and reach local partners in order to state whether additional data could be obtained

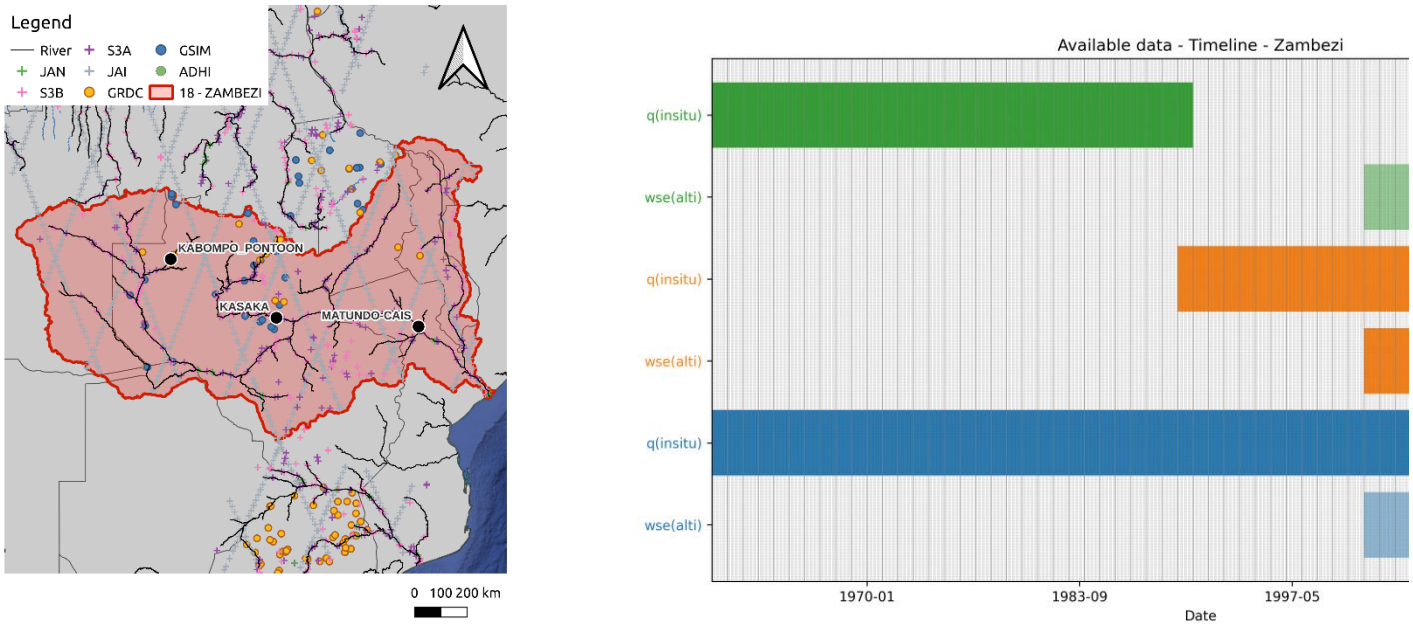

Figure 39. On the left side, the basin (red area) with main drainage network (black line), the available altimetry OLTC data from different constellations (cross) and in-situ gauges stations from different catalogues (colors points). On the right side, timeline of available data (WSE and discharge) for each selected stations of interest.

n°	Station name	River	Country	Lon	Lat	Drainage area (km²)	Period	Timestep	Source
1	KASAKA	KAFUE	ZM	28.216	-15.81	153351	1960-2004	daily	GRDB
2	KABOMPO PONTOON	KABOMPO	ZM	24.216	-13.6	42740	1990-2005	daily	GRDB
3	MATUNDO-CAIS	ZAMBEZE	ZM	33.591	-16.15	940000	1960-1990	daily	GRDB

Table 19. Characteristics of each selected stations with position, river, drainage area, timestep, and period and sources of in-situ gauges.

.

4 Conclusion

Globally, we observe that for most of the basins selected in this activity, there is a good overlap between available in situ data and possible altimetry observations. This will ensure a good quantification of methods errors and uncertainties. However, in some basins, we observe that data availability is poor, and that it will be hard to validate our products. Yet we maintained such stations in the stations list, as they are representative of global basins diversity, and of the requirements from the URD (such as global flow into the ocean). For such stations, we are confident that upstream information on quality will help us provide a discharge time series, with an estimated uncertainty, at the considered location.

As stated above in different basins, the “data availability” is subject to evolution. We put here the “as of today” situation, that may change in function of further discussions with local agencies in the frame of this project or other related ones.

Consequently, this document could be modified during the next year (add stations or new available data after authorization). Any modification will be notified to ESA.

Appendix A -

Annexe A. Basic information concerning daily streamflow databases included in the GSIM project (from Do et al., 2018).

Database (referred name)	Database category	Spatial coverage	Data access information
Global Runoff Data Base (GRDB)	Research database	Global	www.bafg.de/GRDC/ (last access: 23 June 2017) Archived database can be obtained via written request to the Global Runoff Data Centre. This database is updated when new data are submitted by national suppliers.
European Flow Regimes from International Experimental and Network Data (EWA)	Research database	European	http://ne-friend.bafg.de/servlet/is/7413/ (last access: 23 June 2017) Data can be obtained via written request to the Global Runoff Data Centre. This database has been frozen since October 2014 and is being integrated into the GRDB database.
A Regional, Electronic, Hydrographic Data Network for Russia (ARCTICNET)	Research database	Russia	http://www.russia-arcticnet.sr.unh.edu/ (last access: 23 June 2017) Archived and closed historic database. Part of this data archive has been included in the databases of the Global Runoff Data Centre and updated based on data deliveries.
China Hydrology Database Project (CHDP)	Research database	China	http://www.oberlin.edu/faculty/aschmidt (last access: 23 June 2017) Archived and closed historic database can be obtained via written request to the author of the database.
GEOSS ana MAHASRI Experiment in Tropics (GAME)	Research database	Thailand	http://hydro.iis.u-tokyo.ac.jp/GAME-T/GAIN-T/routine/rid-river/disc_d.html (last access: 23 June 2017) Archived and closed historic database
US National Water Information System (USGS)	National database	USA	http://waterdata.usgs.gov/nwis (last access: 23 June 2017) Individual time series can be downloaded from the data portal (updated regularly).
Canada National Water Data Archive (HYDAT)	National database	Canada	https://ec.gc.ca/rhc-wsc/ (last access: 23 June 2017) Archived database. The archive is updated quarterly by the data authority.
Brazil National Water Agency (ANA)	National database	Brazil	http://hidroweb.ana.gov.br/ (last access: 23 June 2017) Individual time series can be downloaded from the data portal (updated regularly).
Japan Water Information System (MLIT)	National database	Japan	http://www1.river.go.jp/ (last access: 23 June 2017) Individual time series can be downloaded from the data portal (updated regularly).
Anuario de aforos digital 2010–2011 (AFD)	National database	Spain	http://ceh-flumen64.cedex.es/anuarioaforos (last access: 23 June 2017) Archived database, DVD available from Spanish authorities (updated annually)
Australia Water Data Online (BOM)	National database	Australia	http://www.bom.gov.au/waterdata/ (last access: 23 June 2017) Individual time series can be downloaded from the data portal (updated regularly).
Water Resources Information System of India (I-WRIS)	National database	India	http://www.india-wris.nrsc.gov.in/wris.html (last access: 23 June 2017) Individual time series can be downloaded from the data portal

References

Ali A. (2013). Indus Basin Floods: Mechanisms, Impacts, and Management. Asian Development Bank, Mandaluyong City, Philippines, ISBN:978-92-9254-284-9.

Aloysius, Noel, and James Saiers. "Simulated hydrologic response to projected changes in precipitation and temperature in the Congo River basin." *Hydrology and Earth System Sciences* 21.8 (2017): 4115-4130.

Alsdorf, Douglas, et al. "Opportunities for hydrologic research in the Congo Basin." *Reviews of Geophysics* 54.2 (2016): 378-409.

ANA - Agência Nacional de Águas (2017). Conjuntura dos Recursos Hídricos do Brasil. Brasília, 2017. Available at: http://www.snirh.gov.br/portal/snirh/centrais-de-conteudos/conjuntura-dos-recursos-hidricos/relatorio-conjuntura-2017.pdf/view.

Bandyopadhyay, J. (1995). Water management in the Ganges-Brahmaputra basin: emerging challenges for the 21st century. *International Journal of Water Resources Development*, *11*(4), 411-442.

Beyer, M., Wallner, M., Bahlmann, L., Thiemig, V., Dietrich, J., & Billib, M. (2016). Rainfall characteristics and their implications for rain-fed agriculture: a case study in the Upper Zambezi River Basin. *Hydrological Sciences Journal*, *61*(2), 321-343.

Biancamaria, S., F. Frappart, A.-S. Leleu, V. Marieu, D. Blumstein, J.-D. Desjonquères, F. Boy, A. Sottolichio, A. Valle-Levinson (2017). Satellite radar altimetry water elevations performance over a 200 m wide river: evaluation over the Garonne River. Advances in Space Research, 59(1), 128-146. http://dx.doi.org/10.1016/j.asr.2016.10.008

Collischonn, W., Allasia, D., da Silva, B. C., & Tucci, C. E. M. (2007). The MGB-IPH model for large-scale rainfall-runoff modelling. *Hydrological Sciences Journal*, *52*(5), 878–895. https://doi.org/10.1623/hysj.52.5.878

Coss, S., Durand, M., Yi, Y., Jia, Y., Guo, Q., Tuozzolo, S., Shum, C. K., Allen, G. H., Calmant, S., and Pavelsky, T. (2020). Global River Radar Altimetry Time Series (GRRATS): new river elevation earth science data records for the hydrologic community. Earth System Science Data, 12, 137-150, https://doi.org/10.5194/essd-12-137-2020

Dargie, Greta C., et al. "Age, extent and carbon storage of the central Congo Basin peatland complex." *Nature* 542.7639 (2017): 86-90.

Diallo, I., Giorgi, F., Deme, A., Tall, M., Mariotti, L., & Gaye, A. T. (2016). Projected changes of summer monsoon extremes and hydroclimatic regimes over West Africa for the twenty-first century. *Climate Dynamics*, *47*(12), 3931–3954. https://doi.org/10.1007/S00382-016-3052-4/FIGURES/12

Do H.X., L. Gudmundsson, M. Leonard, & S. Westra (2018). The Global Streamflow Indices and Metadata Archive (GSIM) - Part 1: The production of a daily streamflow archive and metadata. Earth System Science Data, 10(2), 765-785, https://doi.org/10.5194/essd-10-765-2018

Do, A. T., Sottolichio, A., Huybrechts, N., & Gardel, A. (2020). Circulation patterns and implication for fine sediment transport in a preserved tropical estuary: The case of the Maroni (French Guiana). *Regional Studies in Marine Science*, *40*, 101493.

Espinoza Villar, J. C., Ronchail, J., Guyot, J. L., Cochonneau, G., Naziano, F., Lavado, W., ... & Vauchel, P. (2009). Spatio-temporal rainfall variability in the Amazon basin countries (Brazil, Peru, Bolivia, Colombia, and Ecuador). *International Journal of Climatology: A Journal of the Royal Meteorological Society*, *29*(11), 1574-1594.

FAO (2004). Drought impact mitigation and prevention in the Limpopo River Basin: A Situational Analysis. Land and Water Discussion Paper Vol.4. Food and Agriculture Orgnisation of the United Nations, Rome, Italy.

Fassoni-Andrade, A. C., Fleischmann, A. S., Papa, F., Paiva, R. C. D. D., Wongchuig, S., Melack, J. M., ... & Pellet, V. (2021). Amazon hydrology from space: scientific advances and future challenges. *Reviews of Geophysics*, *59*(4), e2020RG000728.

Furuichi, T., Z. Win, and R. J. Wasson (2009). Discharge and suspended sediment transport in the Ayeyarwady River, Myanmar: Centennial and decadal changes. Hydrological Processes, 23, 1631–1641, doi:10.1002/hyp.7295

Gal, L., Grippa, M., Hiernaux, P., Pons, L., & Kergoat, L. (2017). The paradoxical evolution of runoff in the pastoral Sahel: Analysis of the hydrological changes over the Agoufou watershed (Mali) using the KINEROS-2 model. *Hydrology and Earth System Sciences*, *21*(9), 4591–4613. https://doi.org/10.5194/HESS-21-4591-2017

Gallay, M., Martinez, J. M., Allo, S., Mora, A., Cochonneau, G., Gardel, A., ... & Laraque, A. (2018). Impact of land degradation from mining activities on the sediment fluxes in two large rivers of French Guiana. *Land Degradation & Development*, *29*(12), 4323-4336.

Gao, Huilin, et al. "On the causes of the shrinking of Lake Chad." *Environmental Research Letters* 6.3 (2011): 034021.

Gehring J., B. Duvvuri, and E. Beighley. 2022. Deriving River Discharge Using Remotely Sensed Water Surface Characteristics and Satellite Altimetry in the Mississippi River Basin. Remote Sensing 14(15), 3541, https://doi.org/10.3390/rs14153541

Grill, G., Lehner, B., Thieme, M., Geenen, B., Tickner, D., Antonelli, F., ... & Zarfl, C. (2019). Mapping the world's free-flowing rivers. *Nature*, *569*(7755), 215-221.

de Groen, M. M. and Savenije, H. H. G. (2006). A monthly interception equation based on the statistical characteristics of daily rainfall, Water Resour. Res., 42, W12417, doi:10.1029/2006WR005013.

Gudmundsson L., H.X. Do, M. Leonard, & S. Westra (2018). The Global Streamflow Indices and Metadata Archive (GSIM) - Part 2: Quality control, time-series indices and homogeneity assessment. Earth System Science Data, 10(2), 787-804, https://doi.org/10.5194/essd-10-787-2018

Hastenrath, Stefan, and Stefan Hastenrath. "Climatology of Weather Systems." *Climate and circulation of the tropics* (1985): 210-252.

Heerspink, B. P., Kendall, A. D., Coe, M. T., & Hyndman, D. W. (2020). Trends in streamflow, evapotranspiration, and groundwater storage across the Amazon Basin linked to changing precipitation and land cover. *Journal of Hydrology: Regional Studies*, *32*, 100755.

Jian, J., P. J. Webster, and C. D. Hoyos (2009). Large-scale controls on Ganges and Brahmaputra river discharge on intraseasonal time-scales. Quaterly Journal of the Royal Meteorological Society, 135(639), 353–370, doi:10.1002/qj.384.

Kitambo, B., Papa, F., Paris, A., Tshimanga, R. M., Calmant, S., Fleischmann, A. S., ... & Andriambeloson, J. (2022). A combined use of in situ and satellite-derived observations to characterize surface hydrology and its variability in the Congo River Basin. *Hydrology and Earth System Sciences*, *26*(7), 1857-1882.

Köppen, W., (1900). Versuch einer Klassifikation der Klimate, vorzugsweise nach ihren Beziehungen zur Pflanzenwelt., Geogr. Zeitschr. 6, 593–611, 657–679.

Laraque, Alain, et al. "Evolutions récentes des débits du Congo, de l'Oubangui et de la Sangha." *Geo-Eco-Trop* 37.1 (2013): 93-100.

Latrubesse, Edgardo M., José C. Stevaux, and Rajiv Sinha. "Tropical rivers." *Geomorphology* 70.3-4 (2005): 187-206.

Latrubesse, Edgardo M., et al. "Damming the rivers of the Amazon basin." *Nature* 546.7658 (2017): 363-369.

Lemoalle, J., and Géraud Magrin. "Development of Lake Chad: Current situation and possible outcomes." *IRD Edition, Marseille* (2014).

Kouraev, A. V., Zakharova, E. A., Samain, O., Mognard, N. M., & Cazenave, A. (2004). Ob'river discharge from TOPEX/Poseidon satellite altimetry (1992–2002). Remote sensing of environment, 93(1-2), 238-245.

Lewis J. W., S. E. Lytle, and A. A. Tavakoly (2023). Climate change projections of continental-scale streamflow across the Mississippi River Basin. Theoretical and Applied Climatology, 151, 1013-1034, https://doi.org/10.1007/s00704-022-04243-w

Li, Y., Qin, T., Tun, Y. Y., & Chen, X. (2021). Fishes of the Irrawaddy River: Diversity and conservation. Aquatic Conservation: Marine and Freshwater Ecosystems, 31(8), 1945–1955. https://doi.org/10.1002/AQC.3596

Mahamat, Abdel-Aziz Adam, Adeeba Al-Hurban, and Nehaya Saied. "Change Detection of Lake Chad Water Surface Area Using Remote Sensing and Satellite Imagery." *Journal of Geographic Information System* 13.5 (2021): 561-577.

Mahe, G., Lienou, G., Descroix, L., Bamba, F., Paturel, J. E., Laraque, A., Meddi, M., Habaieb, H., Adeaga, O., Dieulin, C., Chahnez Kotti, F., & Khomsi, K. (2013). The rivers of Africa: witness of climate change and human impact on the environment. *Hydrological Processes*, *27*(15), 2105–2114. https://doi.org/10.1002/HYP.9813

Marengo, J. A. (2005). Characteristics and spatio-temporal variability of the Amazon River Basin Water Budget. *Climate Dynamics*, *24*(1), 11-22.

Miller Z. F., T. M. Pavelsky, and G. H. Allen (2014). Quantifying river form variations in the Mississippi Basin using remotely sensed imagery. Hydrology and Earth System Sciences, 18, 4883-4895, doi: https://doi.org/10.5194/hess-18-4883-2014

Milly P. C. D., and K. A. Dunne (2001). Trends in evaporation and surface cooling in the Mississippi River Basin. Geophysical Research Letters, 28, 1219-1222, https://doi.org/10.1029/2000GL012321

Montanari, A. (2012). Hydrology of the Po River: looking for changing patterns in river discharge. *Hydrology and Earth System Sciences*, *16*(10), 3739-3747.

Mosase, E., & Ahiablame, L. (2018). Rainfall and temperature in the Limpopo river basin, Southern Africa: means, variations, and trends from 1979 to 2013. *Water*, *10*(4), 364.

Nguimalet, C. R., & Orange, D. (2013). Dynamique hydrologique récente de l'Oubangui à Bangui (Centrafrique): impacts anthropiques ou climatiques. Geo-Eco-Trop, 37(1), 101-112.

Nguimalet, C. R. (2017). "Recorded changes over hydrological extremes of Oubangui at Bangui (Central African Republic): trends analysis." Revue des Sciences de l'Eau: Journal of Water Science 30.3: 183-196.

Nguimalet, Cyriaque-Rufin, and Didier Orange. (2019). "Caractérisation de la baisse hydrologique actuelle de la rivière Oubangui à Bangui, République Centrafricaine." La Houille Blanche 1: 78-84.

Nobre, C. A., Obregón, G. O., Marengo, J. A., Fu, R., & Poveda, G. (2009). Characteristics of Amazonian climate: main features. Amazonia and global change, 186, 149-162.

Nones, M., Ronco, P., & Di Silvio, G. (2013). Modelling the impact of large impoundments on the Lower Zambezi River. *International journal of river basin management*, *11*(2), 221-236.

Paiva, R. C. D., Collischonn, W., & Tucci, C. E. M. (2011). Large scale hydrologic and hydrodynamic modeling using limited data and a GIS based approach. Journal of Hydrology, 406(3–4), 170–181. https://doi.org/10.1016/j.jhydrol.2011.06.007

Payne C, Santosh Panda, and Anupma Prakash, Remote Sensing of River Erosion on the Colville River, North Slope Alaska , . Remote Sens. 2018, 10(3), 397; https://doi.org/10.3390/rs10030397.

Peters D.L., T.D. Prowse Regulation effects on the lower Peace River, Canada. Hydrological Processes, 15 (2001), pp. 3181-3194.

Samba, Gaston, and Dominique Nganga. (2012). "Rainfall variability in Congo-Brazzaville: 1932–2007." International Journal of Climatology 32.6: 854-873.

Spencer, Robert GM, et al. (2016). "Origins, seasonality, and fluxes of organic matter in the Congo River." Global Biogeochemical Cycles 30.7: 1105-1121.

Stagl, J. C., & Hattermann, F. F. (2016). Impacts of climate change on riverine ecosystems: alterations of ecologically relevant flow dynamics in the Danube River and its major tributaries. Water, 8(12), 566.

Tarpanelli A., Santi E., Tourian M.J., Filippucci P., Amarnath G., Brocca L. (2019). Daily river discharge estimates by merging satellite optical sensors and radar altimetry through artificial neural network. IEEE Transactions on Geoscience and Remote Sensing, 57(1), 329-341. https://doi.org/ 10.1109/TGRS.2018.2854625

Tarpanelli A., Iodice F., Brocca L., Restano M., Benveniste J. (2020). River flow monitoring by Sentinel-3 OLCI and MODIS: comparison and combination. *Remote Sensing*, 12(23), 3867. https://doi.org/10.3390/rs12233867

Tramblay Y., Rouché N., Paturel J.-E., Mahé G., Boyer J.-F., Amoussou E., Bodian A., Dacosta H., Dakhlaoui H., Dezetter A., Hughes D., Hanich L., Peugeot C., Tshimanga R., Lachassagne P. (2021). ADHI: The African Database of Hydrometric Indices (1950-2018). Earth System Science Data, 13(4), 1547-1560, https://doi.org/10.5194/essd-2020-281

Tourian, M. J., J. T. Reager, and N. Sneeuw. "The total drainable water storage of the Amazon river basin: A first estimate using GRACE." *Water Resources Research* 54.5 (2018): 3290-3312.

Walker HJ, Hudson PF, Hydrologic and geomorphic processes in the Colville River delta, Alaska, Geomorphology 56 (2003) 291–303

Woo, M. K., & Thorne, R. (2003). Streamflow in the Mackenzie basin, Canada. *Arctic*, 328-340.

Woo, M.K., Thorne, R., Winter flows in the Mackenzie drainage system Arctic, 67 (2014), pp. 238-256.

World Bank. (2010). The Zambezi River Basin: A multi-sector investment opportunities analysis. *Modeling, Analysis and Input Data*, *4*, 158.

Yang D., Xiaogang Shi c, Philip Marsh , Variability and extreme of Mackenzie River daily discharge during 1973–2011. Quaternary International Volumes 380–381, 2015, Pages 159-168.

Youssoufa Bele, Mekou, Denis Jean Sonwa, and Anne Marie Tiani. "Supporting local adaptive capacity to climate change in the Congo basin forest of Cameroon: A participatory action research approach." International Journal of Climate Change Strategies and Management 5.2 (2013): 181-197.